The preparation and evaluation of xanthinyl analogues as inhibitors of monoamine oxidase B

Kevin R. Zoellner

B.Pharm.

Dissertation submitted in partial fulfillment of the requirements for the degree Magister Scientiae in Pharmaceutical Chemistry at the North-West University, Potchefstroom Campus

Supervisor:	Dr. J.P. Petzer
Co-supervisor:	Prof. J.J. Bergh
Assistant supervisor:	Prof. S.F. Malan

2006

Potchefstroom

Abstract

Monoamine oxidase B (MAO-B) is a drug target for the treatment of neurodegenerative diseases such as Parkinson's disease. For example, the mechanism-based inactivator of MAO-B, (*R*)-deprenyl, is frequently used in combination with L-dopa as dopamine replacement therapy in Parkinson's disease. In contrast with reversible inhibitors, following treatment with inactivators such as (*R*)-deprenyl, enzyme activity can only be regained via *de novo* synthesis of the MAO-B protein. For this reason, several studies are currently underway to develop safer inhibitors of MAO-B as an alternative to (*R*)-deprenyl. These inhibitors are required to be reversible while retaining selectivity towards MAO-B. We have recently identified (*E*)-8-(3-chlorostyryl)caffeine (CSC) as an exceptionally potent reversible inhibitor of MAO-B with an enzyme-inhibitor dissociation constant (K_i value) of 128 nM.

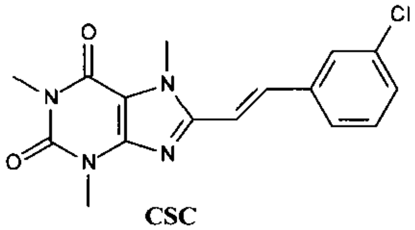

CSC

In an attempt to identify the structural features that are responsible for the high inhibition potency of CSC, we have synthesized six additional analogues of CSC and examined their MAO-B inhibition potencies *in vitro*. The analogues chosen for this study are illustrated below. All of the analogues were found to be reversible inhibitors of baboon liver MAO-B with K_i values in the nano-molar to low micro-molar range.

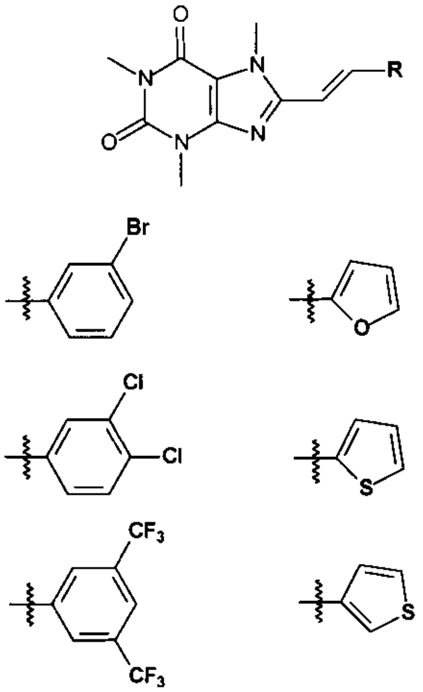

The most potent inhibitor of MAO-B was found to be (*E*)-8-(3,4-dichlorostyryl)caffeine with a K_i value of 36 nM, approximately 3.5 times more potent than the lead compound CSC. (*E*)-8-(3-bromostyryl)caffeine was also found to be a potent inhibitor with a K_i value of 86 nM, also more potent than the lead compound CSC. The thienyl and furyl substituted compounds proved to be moderate inhibitors with K_i values in the low micro-molar range.

Uittreksel

Monoamien oxidase B (MAO-B) is 'n belangrike geneesmiddel teiken vir die behandeling van neurodegeneratiewe siektes soos Parkinson se siekte. Byvoorbeeld, die MAO-B inaktiveerder (*R*)-deprenyl word gereeld gebruik in kombinasie met L-dopa, as dopamien vervangings terapie, vir Parkinsonisme. In kontras met omkeerbare inhibeerders, kan die MAO-B ensiem eers aktiwiteit herwin deur *de novo* sintese van die MAO-B protein, na behandeling met inaktiveerders soos (*R*)-deprenyl. Vir hierdie rede is daar tans verskeie studies onderweg, om veiliger inhibeerders van MAO-B, as alternatief tot (*R*)-deprenyl, te ontwikkel. Hierdie inhibeerders moet omkeerbaar wees, terwyl selektiwiteit vir die MAO-B isoform behou word. (*E*)-8-(3-Chlorostiriel)kaffeien is onlangs geïdentifiseer as 'n besondere potente inhibeerder van MAO-B met 'n ensiem-inhibeerder dissosiasie konstante (K_i waarde) van 128 nM.

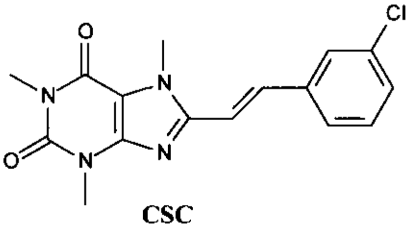

CSC

Om die strukturele eienskappe te identifiseer wat verantwoordelik is vir CSC se hoë inhibisie potensie, het ons additionele analoë van CSC gesintetiseer en hul MAO-B inhibisie potensies *in vitro* ondersoek. Die analoë wat in hierdie studie ondersoek is, word hieronder aangedui. Daar is bevind dat al die analoë wat ondersoek is, inhibisie van MAO-B getoon het , met K_i waardes in die lae nano- en mikro-molaar konsentrasie gebied.

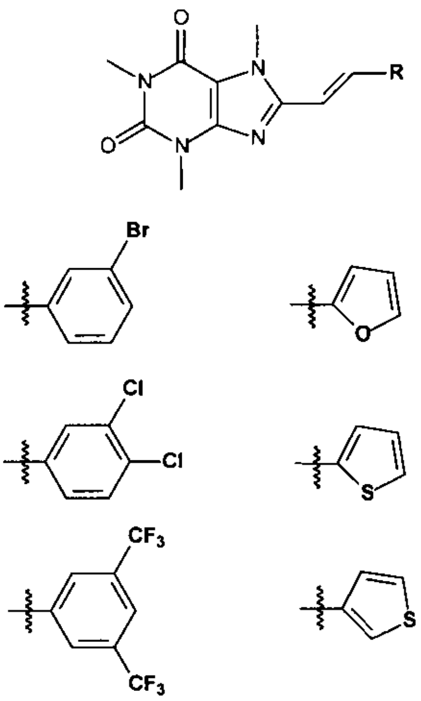

Die (*E*)-8-(3,4-Dichlorostiriel)kaffeien analoog was die potentste van die reeks met 'n K_i-waarde van 36 nM ongeveer 3.5 keer meer potent as die leidraad verbinding CSC. Die tweede potenste verbinding was die (*E*)-8-(3-bromostiriel)kaffeien, met 'n K_i waarde van 86 nM ook meer potent as CSC. Die heterosikliese verbindings was almal middelmatig potente inhibeerders van MAO-B, met K_i waardes in die lae mikro-molaar gebied.

Acknowledgements

This investigation was carried out at the Department of Pharmaceutical Chemistry, North-West University (Potchefstroom campus).

I would like to express my sincere gratitude to the following people and organizations:

- To my supervisor and friend, Dr. J.P. Petzer, for your leadership, patience and encouragement up to the completion of this study. Thank you for sharing your knowledge and guidance with the necessary techniques and skills.
- I would like to thank Prof. J.J. Bergh for his exceptional outlook on life and science. You gave me the chance to participate in important research that will always contribute to my future.
- To Prof. S.F. Malan, for your inspiring ideas and support.
- Prof. Neal Castagnoli for his generous gift of the MMTP used in this study.
- To my father, mother and brother – thank you for your endless support and love that made this journey possible!

Index

Abstract i

Uittreksel iii

Acknowledgements v

Index vi

List of figures ix

Chapter 1: Introduction 11

1.1 Monoamine Oxidase B 11

1.2 Study Aim 13

1.3 Synthetic Pathway 14

1.4 Enzymology 15

1.5 Summary 15

Chapter 2: Synthesis 17

2.1 Preparation of (*E*)-8-styrylcaffeine derivatives 17

2.1.1 The general synthetic approach for 5,6-diamonouracil derivatives 17

2.1.2 Synthetic approaches towards synthesis of caffeine analogues 18

2.1.3 Chemicals and instrumentation 19

2.1.4 1,3-Dimethyl-6-aminouracil (**D**) 19

2.1.5 1,3-Dimethyl-5-nitroso-6-aminouracil (**E**) 20

2.1.6 1,3-Dimethyl-5,6-diaminouracil (**F**) 20

2.1.7 General procedure for the synthesis of (*E*)-8-styrylcaffeinyl analogues (**8a–f**) 20

2.2 Summary 22

Chapter 3: Enzymology 24

3.1 Introduction 24

3.2 Monoamine oxidase 24

3.3 MPTP and Parkinson's disease 25

3.4 Irreversible inhibitors of MAO-B 27

3.5 Reversible inhibitors (Historical background) 27

3.6 MAO-B inhibition and adenosine A_{2A} receptor antagonism 29

3.7 Approaches to the measurement of MAO-B activity *in vitro* 31

3.8 Enzyme kinetics – K_m and V_{max} determination 33

3.9 Enzyme kinetics – K_i determination 35

3.10 Experimental Section 38

3.11 MAO-B incubations for the inhibition studies 38

3.12 Results 39

3.13 Conclusion and Summary 43

Chapter 4: Conclusion 43

References 45

Appendix 53

1.1 (E)-8-(3,5-Ditrifluoromethylstyryl)caffeine ^{1}H-NMR 53

1.2 (E)-8-(3,5-Ditrifluoromethylstyryl)caffeine ^{13}C-NMR 54

1.3 (E)-8-(3,4-Dichlorostyryl)caffeine ^{1}H-NMR 55

1.4 (E)-8-(3,4-Dichlorostyryl)caffeine ^{13}C-NMR ... 56

1.5 (E)-8-(3-Bromostyryl)caffeine ^{1}H-NMR ... 57

1.6 (E)-8-(3-Bromostyryl)caffeine ^{13}C-NMR ... 58

1.7 (E)-8-(2-Thienylethenyl)caffeine ^{1}H-NMR ... 59

1.8 (E)-8-(2-Thienylethenyl)caffeine ^{13}C-NMR ... 60

1.9 (E)-8-(3-Thienylethenyl)caffeine ^{1}H-NMR ... 61

1.10 (E)-8-(3-Thienylethenyl)caffeine ^{13}C-NMR ... 62

1.11 (E)-8-(2-Furylethenyl)caffeine ^{1}H-NMR ... 63

1.12 (E)-8-(2-Furylethenyl)caffeine ^{13}C-NMR ... 64

List of figures

Figure 1-1: The structures of (*R*)-Deprenyl (**1**), Dopamine (**2**) and MPTP (**3**)........................... 11

Figure 1-2: The structures of and rasagiline (**4**), lazabemide (**5**) and safinamide (**6**)............... 12

Figure 1-3: (E)-8-(3-Chlorostyryl)caffeine (CSC) (**7**), the lead compound for this study.. 13

Figure 1-4: The structures of the caffeine analogues that will be examined in this study (**8a–f**).. 14

Figure 1-5: The synthetic pathway to the caffeine analogues that will be examined in this study.. 15

Figure 2-1: Synthetic pathway to 1,3-dimethyl-5,6-diaminouracil (**F**).. 18

Figure 2-2: Synthetic pathway to substituted xanthinyl derivatives... 19

Figure 2-3: Synthetic pathway to the target compounds examined in this study 21

Figure 3-1: Oxidative deamination of dopamine to form toxic metabolites................................ 25

Figure 3-2: The oxidation of MPTP by MAO-B... 26

Figure 3-3: The structures of (*R*)-deprenyl (**1**) and Rasagiline (**4**)... 27

Figure 3-4: The structures of previously reported reversible inhibitors of MAO-B... 28

Figure 3-5: The structures of adenosine A_{2A} receptor antagonists CSC (**7**) and KW-6002 (**18**) 31

Figure 3-6: The oxidation of MMTP (**19**) to form the spectrophotometrically quantifiable MMDP$^+$ (**20**). MMDP$^+$ is stable to further oxidation *in vitro*. 32

Figure 3-7: The oxidation of kynuramine (**21**) by MAO-B and subsequent cyclization to yield 4-hydroxyquinoline (**22**). 33

Figure 3-8: Graphical presentation of the Michealis-Menten equation (V_i versus [S]) 34

Figure 3-9: A Lineweaver-Burke plot (1/ V_i versus 1/[S]). 35

Figure 3-10: Competitive inhibition reaction scheme. 36

Figure 3-11: Lineweaver-Burke plots of a reversible inhibitor with inhibitor concentrations of 0, 10 and 20 μM. 37

Figure 3-12: A graphical illustration of estimating a K_i value from Lineweaver-Burke plots. 37

Figure 3-13: Lineweaver–Burke plots of the oxidation of MMTP by baboon liver MAO-B in the absence (filled circles) and presence of various concentrations of **8e** (open circles, 1 μM; filled triangles, 2 μM; open triangles, 4 μM). The concentration of the baboon liver mitochondrial preparation was 0.15 mg/mL and the rates are expressed as nmoles.mg protein^{-1}.min^{-1} of MMDP^{+} formed. The inset is the replot of the slopes versus the inhibitor concentrations 40

Figure 3-14: Lineweaver–Burke plots of the oxidation of MMTP by baboon liver MAO-B in the absence (filled circles) and presence of various concentrations of **8b** (open circles, 0.1 μM; filled triangles, 0.2 μM; open triangles, 0.4 μM). The concentration of the baboon liver mitochondrial preparation was 0.15 mg/mL and the rates are expressed as nmoles.mg protein^{-1}.min^{-1} of MMDP^{+} formed. The inset is the replot of the slopes versus the inhibitor concentrations 40

Figure 4-1: Structures of *trans,trans-farnesol* (**15**) and isatin (**13**). 43

Introduction

Chapter 1

1.1 Monoamine Oxidase B

Monoamine oxidase (MAO) is a flavin adenine dinucleotide (FAD)-containing enzyme attached to the mitochondrial outer membrane of neuronal, glial, and other cells. Its roles include regulation of the levels of biogenic and xenobiotic amines in the brain and the peripheral tissues by catalyzing their oxidative deamination (Bach *et al.*, 1988). On the basis of their substrate and inhibitor specificities, two types of MAO (A and B) have been described. MAO-A preferentially deaminates serotonin, norepinephrine, and epinephrine (Waldemier, 1987) and is irreversibly inhibited by low concentrations of clorgyline. MAO-B preferentially deaminates β-phenylethylamine and benzylamine and is irreversibly inhibited by (*R*)-deprenyl (**1**) (**Figure 1-1**) (Grimsby *et al.*, 1990). Both isoforms utilize dopamine (**2**) as substrate with MAO-B having the higher catalytic turnover (Youdim & Bakhle, 2006). Due to their role in the metabolism of catecholamine neurotransmitters, MAO-A and –B have long been of considerable pharmacological interest and reversible and irreversible inhibitors of MAO-A and -B have been used clinically to treat neurological disorders including depression and Parkinson's disease (PD) (The Parkinson Study Group, 1989). MAO-B has also been implicated in neurodegenerative processes resulting from exposure to xenobiotic amines. For example, the first step of the bioactivation of the parkinsonian inducing pro-neurotoxin 1-methyl-4-phenyl-1,2,3,6-tetrahydropyridine (MPTP) (**3**) is catalyzed by MAO-B (Chiba *et al.*, 1985a).

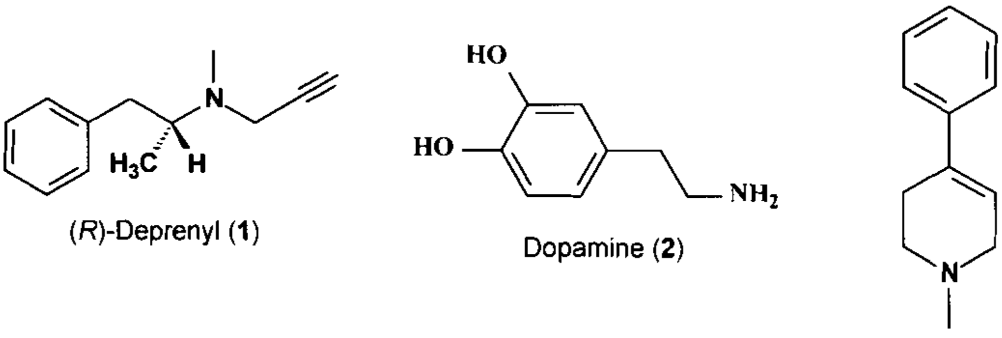

(*R*)-Deprenyl (**1**)

Dopamine (**2**)

MPTP (**3**)

Figure 1-1: The structures of (*R*)-Deprenyl (**1**), Dopamine (**2**) and MPTP (**3**).

MAO-A and –B are therefore important targets for the development of new drugs. We are particularly interested in the therapeutic role of MAO-B inhibitors in the treatment of Parkinson's disease. Since MAO-B is the isoform predominantly responsible for dopamine metabolism in the basal ganglia, inhibition of this enzyme in the brain may conserve the depleted supply of dopamine and inhibitors are frequently used in combination with L-dopa as dopamine replacement therapy in patients diagnosed with early PD (Rabey *et al.*, 2000). For example, MAO-B inhibitors have been shown to elevate dopamine levels in the striatum of primates treated with L-dopa (Finberg *et al.*, 1998). Furthermore, in the catalytic cycle of MAO, one mole of dopaldehyde and H_2O_2 is produced for each mole op dopamine oxidized. Both these catabolic products may be neurotoxic if not rapidly inactivated by centrally located aldehyde dehydrogenase and glutathione peroxidase, respectively. Thus inhibitors of MAO-B may also exert a neuroprotective effect by stoichiometrically decreasing aldehyde and H_2O_2 production in the brain (Youdim & Bakhle, 2006). Inhibitors that have been demonstrated to be of clinical value include the mechanism-based inactivators (*R*)-deprenyl (The Parkinson Study Group, 1989) and rasagiline (**4**) (Rabey *et al.*, 2000) and reversible inhibitors such as lazabemide (**5**) (The Parkinson Study Group, 1996) and safinamide (**6**) (Chazot, 2001) (**Figure 1-2**). From a safety point of view, reversible inhibitors may be therapeutically more desirable than inactivators since MAO-B activity can be regained relatively quickly following withdrawal of the reversible inhibitor. In contrast, return of enzyme activity following treatment with inactivators requires *de novo* synthesis of the MAO-B protein which may require up to two weeks. For this reason, several studies are currently underway to develop reversible inhibitors of MAO-B. These inhibitors act typically in a competitive manner while retaining selectivity towards MAO-B.

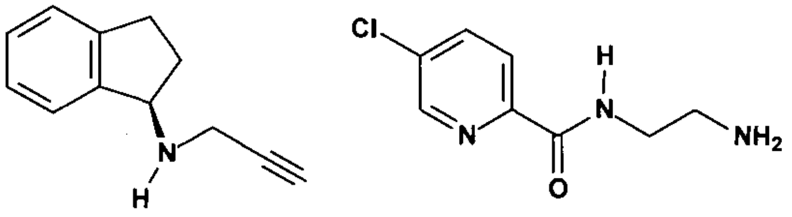

Rasagiline (4) **Lazabemide (5)**

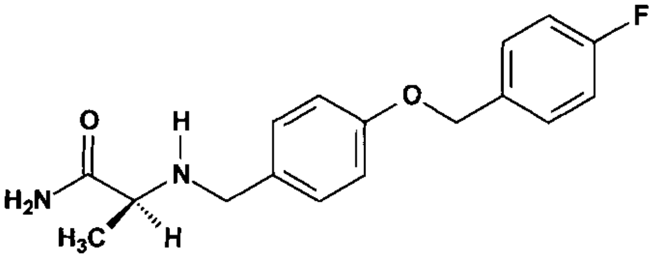

Safinamide (6)

Figure 1-2: The structures of and rasagiline (**4**), lazabemide (**5**) and safinamide (**6**).

We have recently reported that (*E*)-8-styrylcaffeines act as moderate to very potent competitive inhibitors of MAO-B (Petzer *et al.*, 2003). In contrast caffeine only weakly inhibited the enzyme (Chen *et al.*, 2002), which indicates that substitution at C-8 enhances affinity of caffeine analogues for the active site of MAO-B. Substitution at C-8 with an electron deficient styryl functional group produced structures that were especially potent inhibitors. For example, the most potent member of the series was found to be (*E*)-8-(3-chlorostyryl)caffeine (CSC) (**7**) with an enzyme–inhibitor dissociation constant (K_i value) of 128 nM (Vlok *et al.*, 2006). A structure-activity relationship (SAR) study indicated that the structural features important for MAO-B inhibition are the *trans* configuration about the styryl double bond and 1,3,7-trimethyl substitution of the xanthine ring. The literature supports the proposal that wide variety of planar, heterocyclic compounds frequently act as competitive inhibitors of MAO-B. Accordingly a small series of (*E*)-2-styrylbenzimidazoles were shown to be moderate competitive inhibitors of MAO-B (Petzer *et al.*, 2003). In the present study we have examined additional caffeine analogues (**8a–f**) (**Figure 1-4**). in an attempt to identify compounds with improved MAO-B inhibition potency. Among the compounds studied was (*E*)-8-(3-bromostyryl)caffeine (**8a**). Applying a multivariate predictive equation constructed in a previous study (Vlok *et al.*, 2006) this putative inhibitor is predicted to have a K_i value for the inhibition of MAO-B of 106 nM.

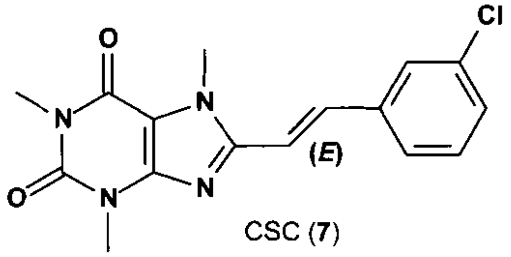

CSC (**7**)

Figure 1-3: (*E*)-8-(3-Chlorostyryl)caffeine (CSC) (**7**), the lead compound for this study.

1.2 Study Aim

In this study we will prepare additional analogues of CSC in an attempt to identify the specific structural features responsible for potent MAO-B inhibition. Earlier studies suggested that structural features important for MAO-B inhibition are the *trans* configuration of the styryl moiety and 1,3,7-trimethyl substitution of the caffeine ring. As part of the present study, the compounds chosen will retain the caffeine core and only differ in substitution at the 8-position of the caffeine ring. All of the compounds chosen will be synthesized and evaluated as reversible inhibitors of MAO-B. The structures (**8a–f**) that will be examined in this study are illustrated in **Figure 1-4**. Among the compounds that will be studied is (*E*)-8-(3-bromostyryl)caffeine (**8a**). Applying a multivariate predictive equation constructed in a previous study (Vlok *et al.*, 2006) this putative inhibitor is predicted to have a K_i value for the inhibition of MAO-B of 106 nM. Also included in this study are analogues substituted at C-8 with 2-furylethenyl (**8d**), 2-thienylethenyl (**8e**) and 3-thienylethenyl (**8f**). A 3-furyl analogue will not be included in this study because the 3-(3-furyl)acrylic acid is not commercially available. These compounds were included in order to determine the influence of electron deficient aromatic rings on MAO-B inhibition activity. We have also included (*E*)-8-styrylcaffeine analogues that are disubstituted on the styryl phenyl ring (**8b** and **8c**).

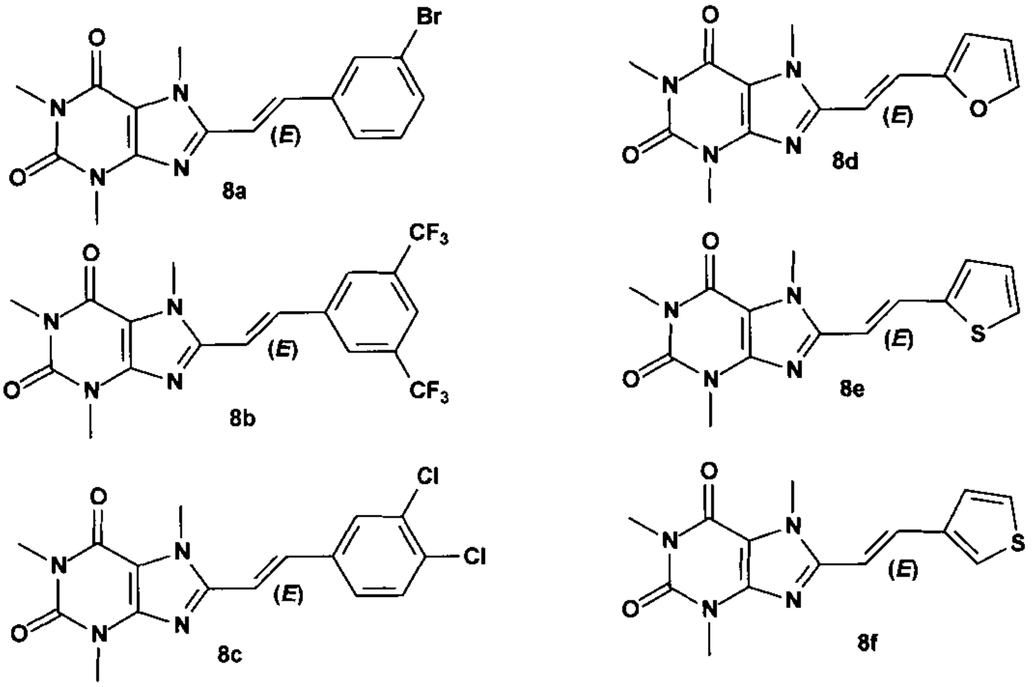

Figure 1-4: The structures of the caffeine analogues that will be examined in this study (**8a–f**).

1.3 Synthetic Pathway

The procedures by which 8-substituted caffeinyl analogues will be synthesized are documented in the literature (Suzuki *et al.*, 1993). Acylation of 1,3-dimethyl-5,6-diaminouracil with an appropriate commercially available carboxylic acid in the presence of a carbodiimide reagent (1-ethyl-2-[3-(dimethylamino)propyl]-carbodiimide, EDAC) followed by treatment with sodium hydroxide results in the corresponding 1,3-dimethyl-7*H*-xanthinyl analogues. These reaction intermediates will be 7N-methylated in the presence of an excess of iodomethane and potassium carbonate to yield the target compounds. Following recrystallization from a suitable solvent the structures and purity of the compounds will be verified by mass spectrometry and NMR. The trans geometry about the double bond will confirmed by a proton-proton coupling constants which are in the range of 15-16 Hz.

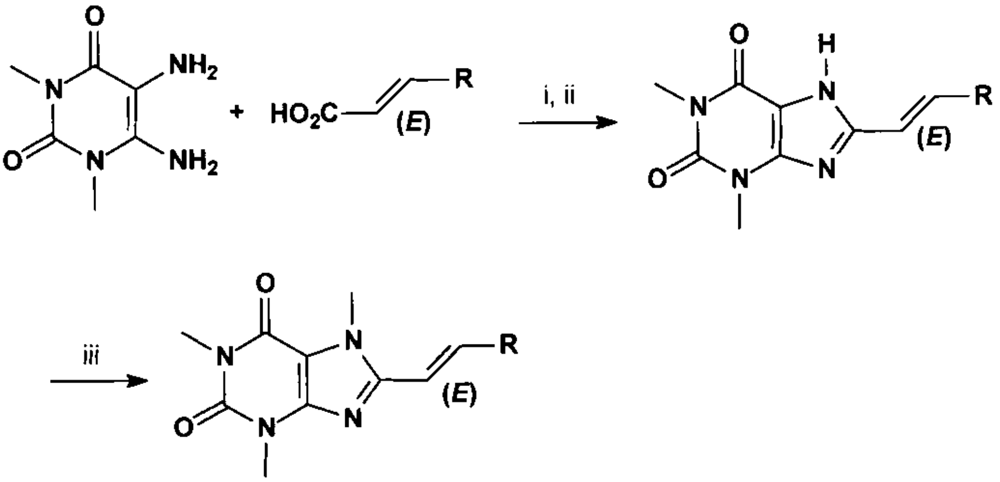

Figure 1-5: The synthetic pathway to the caffeine analogues that will be examined in this study. Key: (i) EDAC; (ii) NaOH; (iii) CH_3I, K_2CO_3.

1.4 Enzymology

As source of MAO-B we will use the mitochondrial fraction from baboon liver tissue. MAO-B from baboon liver is reported to have approximately the same inhibitor specificities as MAO-B obtained from human liver (Hubálek *et al.*, 2005). Because of its ease of operation we will employ spectrophotometry to measure MAO-B activity. As enzyme substrate we routinely use 1-methyl-4-(1-methylpyrrol-2-yl)-1,2,3,6-tetrahydropyridine (MMTP) (Vlok *et al.*, 2006). Each incubation will contain MAO-B (0.15 mg/mL of the mitochondrial fraction), MMTP (30-120 µM) and various concentrations of the test inhibitor dissolved in sodium phosphate buffer. Following a 15 minute incubation period the reactions will be terminated by the addition of perchloric acid and the concentration of $MMDP^+$ (the oxidation product of MMTP) will be measured spectrophotometrically at a wavelength of 420 nm. K_i values are obtained from a replot of the slopes of the Lineweaver-Burke plots vs. the inhibitor concentration (Vlok *et al.*, 2006).

1.5 Summary

Idiopathic Parkinson's disease (PD) is a neurological disorder, characterized by the marked loss of dopaminergic nigrostriatal neurons, and clinically by disabling movement disorders. Treatment for PD relies on replacement of diminished dopamine stores, via treatment with L-dopa. MAO-B inhibitors have also been shown to be of value in the treatment of PD. Currently irreversible inhibitors of MAO-B, such as (*R*)-deprenyl are most frequently used for the treatment of PD. Because of safety considerations, reversible inhibitors may be more desirable as a treatment strategy. Our approach to developing novel inhibitors of MAO-B is based on previous studies with the reversible MAO-B inhibitor, (*E*)-8-(3-chlorostyryl)caffeine (CSC) (**7**) (**Figure 1-3**). SAR studies indicated that the *trans* configuration, and 1,3-7-trimethyl substitution of the caffeine ring, are important for potent inhibitory effect. Based on this knowledge six derivatives, of CSC will be synthesized, and their enzyme dissociation constants (K_i values) will be determined.

Synthesis

Chapter 2

2.1 Preparation of (*E*)-8-styrylcaffeine derivatives

Substitution of caffeine with a (*E*)-styryl functional group at the 8 position results in compounds that are exceptionally potent reversible inhibitors of MAO-B. Using standard literature procedures (Suzuki *et al.*, 1993; Jacobson *et al.*, 1993; Müller *et al.*, 1997a) six 8-substituted caffeine derivatives were prepared in this study.

2.1.1 The general synthetic approach for 5,6-diamonouracil derivatives

For the synthesis of caffeine derivatives most of the reported methods make use of 5,6-diaminouracil (**F**) as starting material. 5,6-Diaminouracil can be prepared according to a general procedure first described by Traube (1900) in which a symmetric dimethylurea (**A**) is condensed with cyanoacteic acid (**B**) in the presence of acetic anhydride (**i**) to yield a cyanoacetylurea intermediate (**C**) (**Figure 2-1**). On treatment with aqueous sodium hydroxide (Papesch & Schroeder, 1951) or a metal alkoxide base (**ii**) (Triplett *et al.*, 1978) ring closure takes place to form 1,3 dimethyl-6-aminouracil (**D**). When **D** is treated with sodium nitrite in the presence of an acid (**iii**), 1,3-dimethyl-5-nitroso-6-diaminouracil (**E**) is formed which can be reduced to the desired 5,6-diaminouracil (**F**) with sodium hydrosulfite (**iv**) (Blicke & Godt, 1954; Speer & Raymond, 1953).

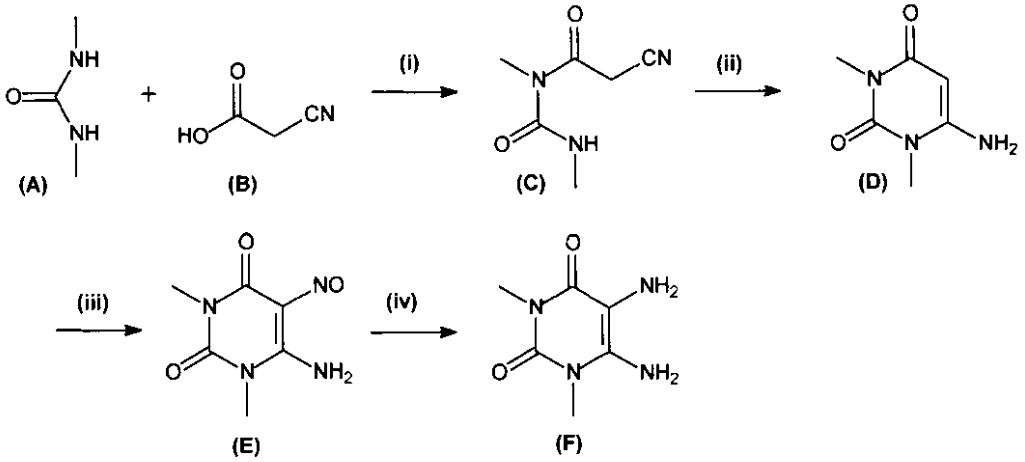

Figure 2-1: Synthetic pathway to 1,3-dimethyl-5,6-diaminouracil (**F**). Key: (i) acetic anhydride. (ii) NaOH (aq) or NaOEt. (iii) $NaNO_2$, CH_3CO_2H. (iv) $Na_2S_2O_4$.

2.1.2 Synthetic approaches towards synthesis of caffeine analogues

For the synthesis of substituted caffeine analogues most literature procedures make use a 5,6-diaminouracil derivative (**F**) as key starting material (**figure 2-2**) (Shimada *et al.*, 1992; Müller *et al.*, 1997a; Suzuki *et al.*, 1993). Acylation of the uracil (**F**) with a carboxylic acid followed by treatment with aqueous sodium hydroxide give the corresponding 7H-xanthinyl derivative (**I**) (Shimada *et al.*, 1992). A commercial carbodiimide reagent is used to convert the carboxylic acid to the active acylation agent. The carbodiimide most frequently used is 1-ethyl-3-[3-(dimethylamino-propyl]carbodiimide (EDAC) (Müller *et al.*, 1997). Another approach to this reaction has been documented by Jacobson *et al.*, (1993). The uracil (**F**) is acylated by an acid chloride in pyridine as solvent (Shimada *et al.*, 1992; Müller *et al.*, 1997a). The amide intermediate (**G**) can be cyclisized by treating with phosphorous oxychloride or aqueous sodium hydroxide (Shimada *et al.*, 1992). Condensation of an aldehyde with the uracil (**F**) is also frequently reported. The product an imine (**H**), is subsequently subjected to oxidative ring closure using ferric chloride or thienyl chloride (**vii**). Most frequently methylation of the 7-N position (**J**) is required for potent inhibition of the MAO-B enzyme. This is achieved by addition of iodomethane in the presence of a weak base such as potassium carbonate (**ix**).

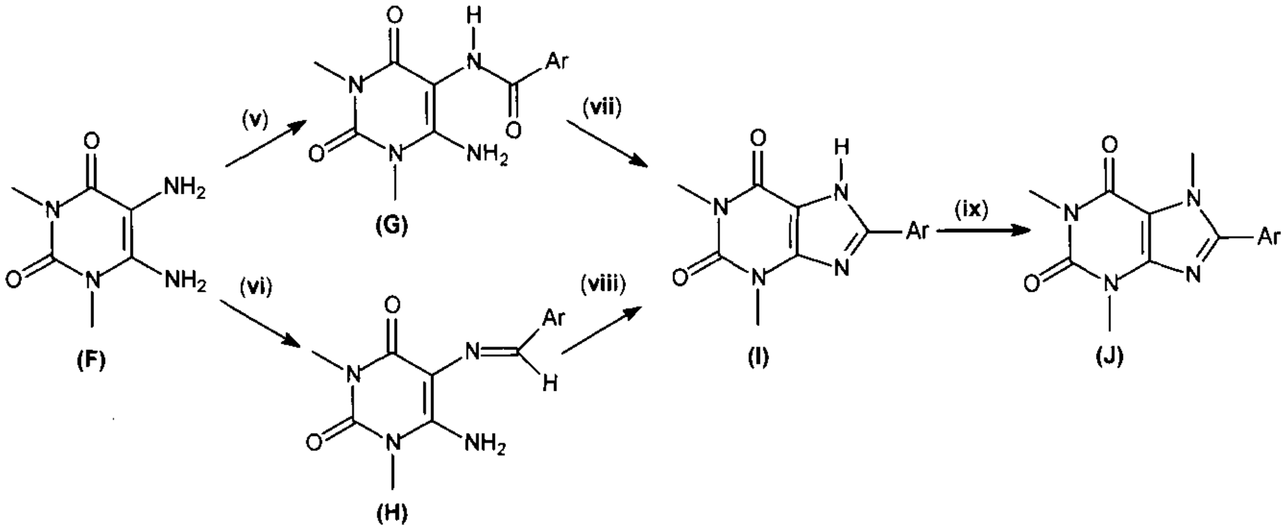

Figure 2-2: Synthetic pathway to substituted xanthinyl derivatives. Key: (v) ArCOCl pyridine or $ArCO_2H$, 1-ethyl-3-[3-(dimethylamino)-propyl]carbodiimide (EDAC). (vi) ArCHO, acetic acid. (vii) NaOH (aq), reflux or $POCl_3$, reflux. (viii) $FeCl_3$, reflux or $SOCl_2$. (ix) CH_3I, K_2CO_3.

2.1.3 Chemicals and instrumentation

All starting materials not described elsewhere were obtained from Sigma-Aldrich and were used without purification. Proton and carbon NMR spectra were recorded on a Varian Gemini 300 spectrometer. Proton (^1H) spectra were recorded in $CDCl_3$ at a frequency of 300 MHz and carbon (^{13}C) spectra at 75 MHz. Chemical shifts are reported in parts per million (δ) downfield from the signal of tetramethylsilane added to the deuterated solvent. Spin multiplicities are given as s (singlet), d (doublet), t (triplet), q (quartet) or m (multiplet) and the coupling constants (*J*) are given in hertz (Hz). Direct insertion electron impact ionization (EIMS) and high resolution mass spectra (HRMS) were obtained on a VG 7070E mass spectrometer. Melting points (mp) were determined on a Gallenkamp melting point apparatus. All the melting points are uncorrected. Thin layer chromatography (TLC) was carried out using silica gel 60 (Macherey-Nagel) containing UV_{254} fluorescent indicator.

2.1.4 1,3-Dimethyl-6-aminouracil (D)

1,3-Dimethylurea (**A**) (55 mmol) and cyanoacetic acid (**B**) (55 mmol) were dissolved in 7.1 mL acetic anhydride with the exclusion of moisture (anhydrous calcium chloride trap). After the mixture was heated and stirred at 60 °C for 3 to 5 hours the excess anhydride and acetic acid were removed under reduced pressure, to yield a light yellow oil (**C**). Slow addition of an aqueous sodium hydroxide solution (5 %) to the stirred residue on ice resulted in the formation of 1,3-

dimethyl-6-aminouracil (**D**) as precipitate, which was collected by filtration. The reaction was monitored using silica gel thin layer chromatography with 100 % methanol, as mobile phase. **Yield** 81.5 %; **MP** 188 °C, literature, 198-199 °C (Papesch & Schroeder, 1951).

2.1.5 1,3-Dimethyl-5-nitroso-6-aminouracil (E)

A solution of sodium nitrite (36 mmol) in 15 mL water was added to **D** (30 mmol) suspended in 30 mL water and the mixture was acidified by the dropwise addition of 3.6 mL aqueous acetic acid (36 %) over a period of one hour. Stirring was continued for an additional 3 hours at room temperature. After cooling to 0 °C, the violet precipitate (**E**) was isolated by filtration and washed with water. Compound **E** was obtained in a **yield** of 95 % **mp** >240 °C, literature, 233 °C (Blicke & Godt, 1954).

2.1.6 1,3-Dimethyl-5,6-diaminouracil (F)

1,3-Dimethyl-5-nitroso-6-aminouracil (**E**) (16.4 mmol) was suspended in 16.4 mL ammonia water (30 %) to yield a yellow orange suspension. While heating the suspension at 40 °C, sodium hydrosulfite (51.9 mmol) in 7.2 mL distilled water, was added portionwise over a period of 20 minutes. Stirring was continued for another 30 minutes. The reaction turned into a light yellow solution which was cooled on ice. The product (**F**) crystallized from solution and was collected by filtration. This reaction was monitored using thin layer chromatography with 100% methanol as mobile phase. (**F**) Was obtained in a **yield** of 85 % **mp** 206 °C, literature 209 °C (Blicke & Godt, 1954).

2.1.7 General procedure for the synthesis of the (*E*)-8-styrylcaffeinyl analogues (8a–f)

The (*E*)-8-styrylcaffeine analogues (**8a–f**) examined in this study were prepared according to the procedure described by Suzuki and co-workers (Suzuki *et al.*, 1993). 1,3-Dimethyl-5,6-diaminouracil (**F**, 3.50 mmol) and 1-ethyl-2-[3-(dimethylamino)propyl]-carbodiimide hydrochloride (EDAC; 5.11 mmol) was dissolved in 40 mL dioxane:H_2O (1:1) followed by the addition of the appropriate commercially available carboxylic acid (3.81 mmol). The pH of the suspension was adjusted to 5 with 2 M aqueous hydrochloric acid and stirring was continued for an additional 2 hours. The reaction was neutralized with 1 M aqueous sodium hydroxide, cooled to 0 °C and the resulting precipitate was collected by filtration. The crude product was dissolved in 40 mL aqueous sodium hydroxide (1 M):dioxane (1:1) and heated for 2 hours under reflux. The reaction solution was cooled to 0 °C, acidified to a pH of 4 with 4 M aqueous hydrochloric acid and the precipitate was collected by filtration (**I**). The resulting 8-substituted analogues (**I**) were reacted in the subsequent reaction without further purification. Iodomethane (0.40 mmol) was added to a stirred suspension of **I** (0.20 mmol) and potassium carbonate (0.50 mmol) in 5 mL DMF (**ix**). Stirring was continued at 60 °C for 60 minutes, the insoluble materials were removed by filtration and sufficient water was added to the filtrate to precipitate the product (**8a–f**) that was collected by filtration. Following recrystallization from a mixture of methanol:ethyl acetate (9:1) analytically pure samples of **8a–f** were obtained. For previously reported **8e** we found the melting point to be 218 °C while the reported melting point is 216–218 °C (Del Guidice *et al.*, 1996). NMR and MS data also correlated to that described.

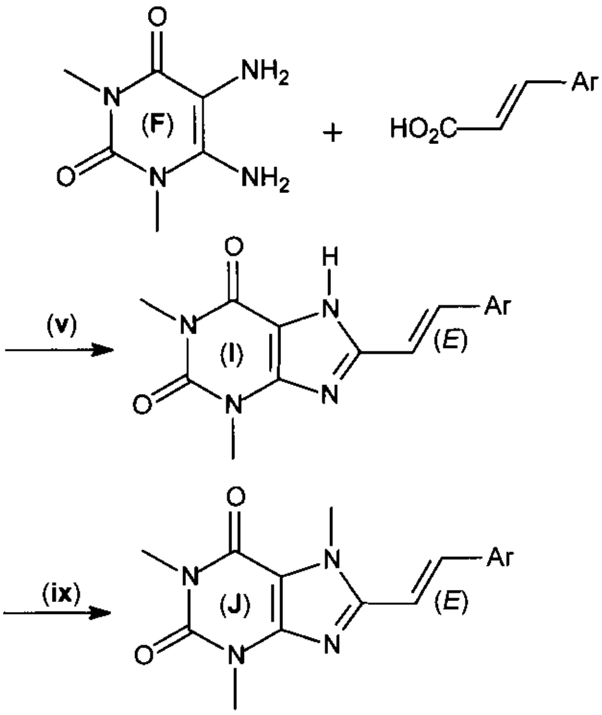

Figure 2-3: Synthetic pathway to the target compounds examined in this study. Key: (**v**) 1-ethyl-3-[3-(dimethylamino)-propyl]carbodiimide (EDAC), NaOH, reflux (**ix**) CH_3I, K_2CO_3.

(E)-8-(3-Bromostyryl)caffeine (**8a**) was prepared from 1,3-dimethyl-5,6-diaminouracil (**F**) and *trans*-3-bromocinnamic acid in a yield of 37 %: mp > 240 °C (capillary method); ^{1}H NMR ($CDCl_3$) δ 3.38 (s, 3H), 3.59 (s, 3H), 4.05 (s, 3H), 6.88(d, 1H, *J* = 15.8 Hz), 7.25 (m, 1H), 7.45(dd, 2H, *J* = 1.7, 7.9 Hz), 7.70 (d, 1H, *J* = 15.7Hz), 7.71 (t, 1H, *J* = 1.8 Hz); ^{13}C NMR ($CDCl_3$) δ 27.92, 29.72, 31.55, 108.12, 112.59, 123.12, 126.16, 129.81, 130.42, 132.21 , 136.48, 137.64, 148.52, 149.30, 151.65, 155.24; EIMS *m/z* 374 and 376 (M^+); HRMS calcd. 374.0378, found 374.0371.

(E)-8-(3,5-Ditrifluoromethylstyryl)caffeine (**8b**) was prepared from 1,3-dimethyl-5,6-diaminouracil (**F**) and *trans*-3,5-ditrifluoromethylcinnamic acid in a yield of 38 %: mp 238 °C (capillary method); ^{1}H NMR ($CDCl_3$) δ 3.39 (s, 3H), 3.60 (s, 3H), 4.10 (s, 3H), 7.03 (d, 1H, *J* = 15.8 Hz), 7.82 (bs, 1H),

7.84 (d, 1H, J = 15.8 Hz), 7.96 (bs, 2H); ^{13}C NMR ($CDCl_3$) δ 27.96, 29.71, 31.70, 108.49, 114.84, 122.42, 124.89, 126.90, 132.48 (q), 134.53, 137.62, 148.44, 148.47, 151.60, 155.25; EIMS *m/z* 432 (M^+); HRMS calcd. 432.1021, found 432.1001.

(E)-8-(3,4-Dichlorostyryl)caffeine (**8c**) was prepared from 1,3-dimethyl-5,6-diaminouracil (**F**) and *trans*-3,4-dichlorocinnamic acid in a yield of 42 %: mp > 240 °C (capillary method); ^{1}H NMR ($CDCl_3$) δ 3.39 (s, 3H), 3.60 (s, 3H), 4.06 (s, 3H), 6.87 (d, 1H, J = 15.7 Hz), 7.37(m, 1H), 7.45 (d, 1H, J = 8.4 Hz), 7.64 (d, 1H, J = 2.1 Hz), 7.68 (d, 1H, J = 15.7 Hz); ^{13}C NMR ($CDCl_3$) δ 27.93, 29.72, 31.56, 108.18, 112.91, 126.46, 128.68, 130.89, 133.24, 133.28, 135.40, 135.57, 148.49, 149.07, 151.62, 155.22; EIMS *m/z* 365 (M^+); HRMS calcd. 364.0494, found 364.0513.

(E)-8-(2-Furylethenyl)caffeine (**8d**) was prepared from 1,3-dimethyl-5,6-diaminouracil (**F**) and 3-(2-furyl)acrylic acid in a yield of 35 %: mp > 240 °C (capillary method); ^{1}H NMR ($CDCl_3$) δ 3.35 (s, 3H), 3.56 (s, 3H), 3.98 (s, 3H), 6.44 (m, 1H), 6.52 (d, 1H, J = 3.92 Hz), 6.75 (d, 1H, J = 15.5 Hz), 7.44 (d, 1H, J = 2.3 Hz), 7.72 (d, 1H, J = 6.32 Hz), 7.50 (d, 1H, J = 15.5 Hz); ^{13}C NMR ($CDCl_3$) δ 27.84, 29.63, 31.37, 107.86, 109.11, 112.34, 113.12, 124.63, 143.87, 148.55 , 149.86, 151.63, 151.79, 155.08; EIMS *m/z* 286 (M^+); HRMS calcd. 286.1066, found 286.1064.

(E)-8-(2-Thienylethenyl)caffeine (**8e**) was prepared from 1,3-dimethyl-5,6-diaminouracil (**F**) and 3-(2-thienyl)acrylic acid in a yield of 32 %: mp 204 °C (capillary method); ^{1}H NMR ($CDCl_3$) δ 3.36 (s, 3H), 3.57 (s, 3H), 3.99 (s, 3H), 6.63 (d, 1H, J = 15.4 Hz), 7.03 (dd, 1H, J = 5.1, 5.1 Hz), 7.21 (d, 1H, J = 4.8 Hz), 7.30 (d, 1H, J = 5.1 Hz), 7.86 (d, 1H, J = 15.4 Hz); ^{13}C NMR ($CDCl_3$) δ 27.86, 29.67, 31.44, 107.82, 110.21, 127.02, 128.14, 129.46, 130.89, 140.84, 148.53, 149.65, 151.62, 155.09; EIMS *m/z* 302 (M^+); HRMS calcd. 302.0837, found 302.0820.

(E)-8-(3-Thienylethenyl)caffeine (**8f**) was prepared from 1,3-dimethyl-5,6-diaminouracil (**F**) and 3-(3-thienyl)acrylic acid in a yield of 35 %: mp 218 °C (capillary method), literature mp 216–218 °C (Del Guidice *et al.*, 1996) ; ^{1}H NMR ($CDCl_3$) δ 3.36 (s, 3H), 3.57 (s, 3H), 3.99 (s, 3H), 6.68 (d, 1H, J = 15.5 Hz), 7.32 (m, 2H), 7.44 (dd, 1H, J = 1.9, 2.4 Hz), 7.75 (d, 1H, J = 15.6 Hz); ^{13}C NMR ($CDCl_3$) δ 27.84, 29.67, 31.41, 107.80, 110.98, 124.61, 126.27, 126.91, 132.06, 138.47, 148.50, 150.01, 151.62, 155.11; EIMS *m/z* 302 (M^+); HRMS calcd. 302.0837, found 302.0830.

2.2 Summary

Following literature procedures, six (*E*)-8-styrylcaffeine derivatives were prepared. With the exception of **8e**, all of the compounds are previously unknown. The identities and purities of the prepared compounds were confirmed by mass, ^{1}H NMR and ^{13}C NMR spectroscopy. The *trans* geometry about the styryl double bonds of **8a–f** were confirmed by proton-proton coupling constants which were in the range of 15.4–15.8 Hz for the olefinic proton signals.

Enzymology

Chapter

3

3.1 Introduction

Degeneration of nigrostriatal dopamine neurons is the main pathological cause of Parkinson's disease. A definitive neuropathological diagnosis of Parkinson's disease requires loss of dopaminergic neurons in the substantia nigra and related brain stem nuclei, and the presence of Lewy bodies in remaining nerve cells (Youdim *et al.*, 2005). The contribution of genetic factors to the pathogenesis of Parkinson's disease is increasingly being recognized. A point mutation which is sufficient to cause a rare autosomal dominant form of the disorder has been recently identified in the alpha-synuclein gene on chromosome 4 in the much more common sporadic, or 'idiopathic' form of Parkinson's disease, and a defect of complex I of the mitochondrial respiratory chain was confirmed at the biochemical level. Disease specificity of this defect has been demonstrated for the parkinsonian substantia nigra (Ebadi *et al.*, 2001).

Treatment approaches remain to enhance dopaminergic flux, limiting of toxic byproducts and the action of dopamine agonists. Monoamine oxidase B (MAO-B) is therefore a drug target for the treatment of neurodegenerative diseases such as Parkinson's disease (Rabey *et al.*, 2000).

3.2 Monoamine oxidase

Monoamine oxidase (MAO) is an enzyme responsible for the oxidative deamination of various physiologically and pathologically important monoamine neurotransmitters and hormones such as dopamine (**Figure 3-1**), noradrenaline, adrenaline, and serotonin (Nagatsu, 2004). Inhibitors of Complex I of the mitochondrial respiratory chain, such as rotenone, and MPTP, promote Parkinson disease-like symptoms and signs of oxidative stress. Dopamine (DA) oxidation products may be implicated in such a process (Zoccarato *et al.*, 2005).

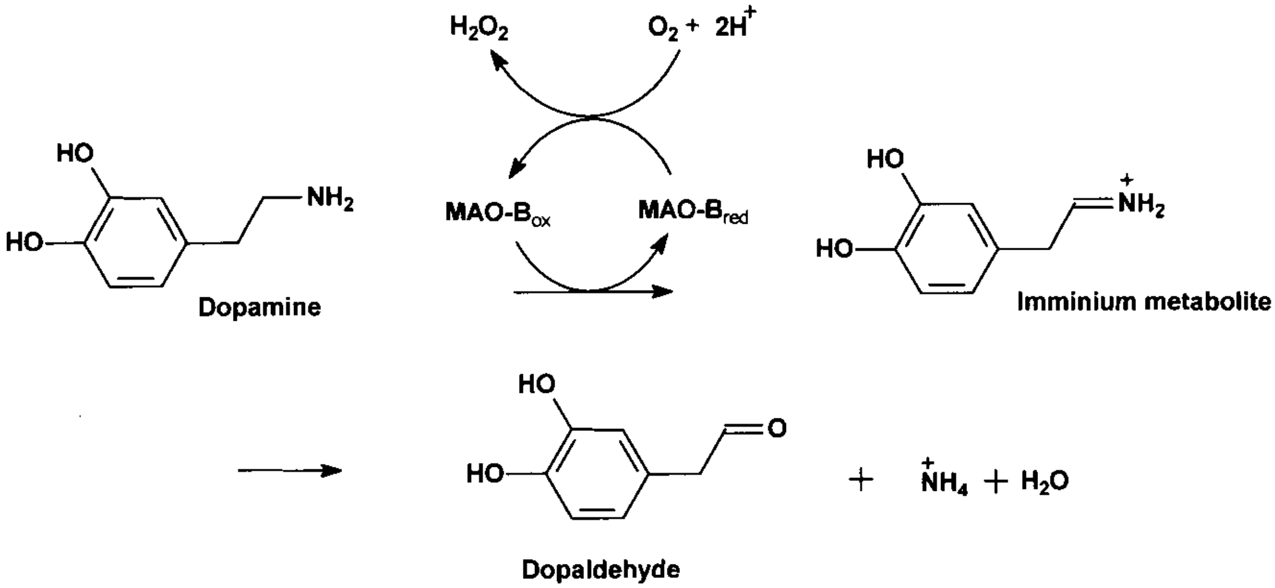

Figure 3-1: Oxidative deamination of dopamine to form toxic metabolites.

The enzyme exists in two distinct isoforms, A and B. MAO-A is inhibited by clorgyline and MAO-B, by (*R*)-deprenyl. cDNA of MAO-A and MAO-B were cloned and their structures determined. MAO-A and MAO-B are encoded by different nuclear genes located on the X chromosome (Xp11.23). MAO-A and MAO-B genes consist of 15 exons with identical intron-exon organization, suggesting that they were derived from a common ancestral gene. Both enzymes require a flavin cofactor, flavin adenine dinucleotide (FAD), which binds to the cysteine residue of a pentapeptide sequence (Ser-Gly-Gly-Cys-Tyr) (Nagatsu, 2004). Both enzymes exist on the outer membrane of mitochondria of various types of cells in various tissues including the brain. In humans, MAO-B is abundant in the brain and liver, whereas the liver, lungs and intestine are rich in MAO-A. MAO-A oxidizes noradrenaline and serotonin while MAO-B mainly utilizes beta-phenylethylamine as substrate. In the human brain, MAO-A exists in catecholaminergic neurons, but MAO-B is found in serotonergic neurons and glial cells. MAO-A knockout mice exhibit increased serotonin levels and aggressive behavior, whereas MAO-B knockout mice show little behavioral change. MAO-A and MAO-B may be closely related to various neuropsychiatric disorders such as depression and Parkinson's disease, and inhibitors of them are the subject of drug development for such diseases (Nagatsu, 2004)

3.3 MPTP and Parkinson's disease

The enzyme monoamine oxidase B (MAO-B) has been identified as the principal enzyme responsible for the metabolic activation of the proneurotoxin 1-methyl-4-phenyl-1,2,3,6-tetrahydropyridine (MPTP) (**3**) in the brains of mammals including humans (**Figure 3-2**) (Chiba *et al.*, 1984). The molecular mechanisms by which MPTP selectively damages nigrostriatal neurons and induces a parkinsonian syndrome in mammals, including humans, has been the subject of extensive research (Heikkila *et al.*, 1984a). Critical to its mode of action is the MAO-B catalyzed α-carbon oxidation of the parent compound yielding the corresponding 1-methyl-4-phenyl-2,3-dihydropyridinium species MPDP$^+$ (**9**). This metabolic intermediate undergoes a second two-electron oxidation to generate the 1-methyl-4-phenylpyridinium metabolite MPP$^+$ (**10**), the ultimate neurotoxin (Chiba *et al.*, 1984).

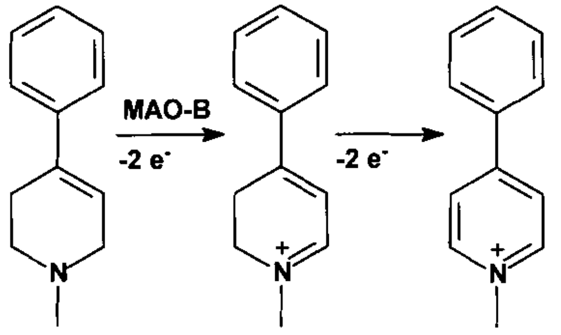

MPTP (3) **MPDP$^+$(9)** **MPP$^+$(10)**

Figure 3-2: The oxidation of MPTP by MAO-B.

This process appears to take place mainly in glial cells where MAO-B is located (Takada *et al.*, 1990). MPP$^+$ is believed to be transported into the nigrostriatal dopaminergic nerve terminals, possibly via the plasma membrane dopamine transporter (DAT) where it localizes within the inner mitochondrial membrane. Inhibition of complex I of the mitochondrial respiratory chain by MPP$^+$ leads to downstream events such as ATP depletion and oxidative stress which eventually result in degeneration of nigrostriatal dopaminergic neurons. The remarkable selectivity of MPP$^+$ as a nigrostriatal toxin can presumably be explained by the ability of the DAT system to actively concentrate MPP$^+$ in the dopaminergic neuron (Chiba *et al.*, 1985b). Experimental animals treated with MPTP have become useful models for studying neurodegenerative processes. In a frequently used protocol the striatal dopamine concentrations of C57BL/6 mice are measured seven days following systemic injection (multiple or single doses) of MPTP (Schmidt & Ferger, 2001). MPP$^+$ induced depletion of striatal dopamine is indicative of the permanent loss of nigrostriatal dopaminergic cell bodies in the substantia nigra. Nigrostriatal cell death in 1-methyl-4-phenyl-1,2,3,6-tetrahydropyridine (MPTP)-induced Parkinson's disease, therefore arises from the pyridinium metabolite [1-methyl-4-phenylpyridinium (MPP$^+$)], formed by the MAO-B catalyzed oxidation of MPTP.

3.4 Irreversible inhibitors of MAO-B

(*R*)-Deprenyl (**1**) (**Figure 3-3**) gained wide acceptance as a useful form of adjunct with L-dopa as therapy for Parkinson's disease (Nyholm, 2006). The effect of L-dopa is potentiated and prolonged by (*R*)-deprenyl (Heinonen & Rinne, 1989). (*R*)-Deprenyl belongs to the class of enzyme-activated irreversible inhibitors, because it acts as substrate for the target enzyme, whose action on the compound results in irreversible inhibition.

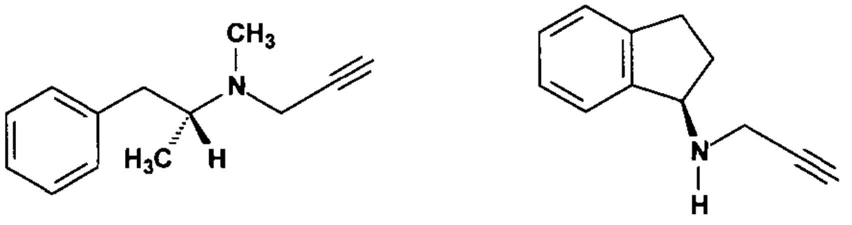

(*R*)-Deprenyl (1) **Rasagiline (4)**

Figure 3-3: The structures of (*R*)-deprenyl (**1**) and rasagiline (**4**).

(*R*)-Deprenyl first of all forms a noncovalent complex with MAO as an initial, reversible step. Inhibitor-enzyme interaction leads to a reduction of the enzyme-bound flavin-adenine dinucleotide (FAD), and concomitant oxidation of the inhibitor. This oxidized inhibitor then reacts with FAD at the N-5-position in a covalent manner, to form a deactivated MAO-B-deprenyl combination. The observed *in vitro* selectivity of (*R*)-deprenyl for MAO-B may be accounted for by differences in the affinities of the two MAO subtypes for reversible interaction with (*R*)-deprenyl, differences in the rates of reaction within the noncovalent complexes to form the irreversibly inhibited adduct, or a combination of both these factors (Gerlach *et al.*, *1992)*. Examination of different derivatives of the suicide inhibitors showed that the propargyl moiety is essential to the neuroprotective effect of these molecules (Palfi *et al.*, 2006; Bonneh-Barkay *et al.*, 2005; Youdim *et al.*, 2005). (*R*)-Deprenyl (**1**) and rasagiline (**4**) (**Figure 3-3**) also markedly attenuate the neurotoxic effects of MPTP (Kupsch *et al.*, 2001).

3.5 Reversible inhibitors

From a safety point of view, reversible inhibitors may be therapeutically more desirable than inactivators since MAO-B activity can be regained relatively quickly following withdrawal of the reversible inhibitor. In contrast, return of enzyme activity following treatment with inactivators requires *de novo* synthesis of the MAO-B protein which may require up to two weeks. For this reason, several studies are currently underway to develop reversible inhibitors of MAO-B. These inhibitors act typically in a competitive manner while retaining selectivity towards MAO-B. Examples of reversible inhibitors of MAO-B that are reported in the literature are shown in (**Figure 3-4**). Their potencies, mode of action and type of enzyme used are indicated in **Table 1**.

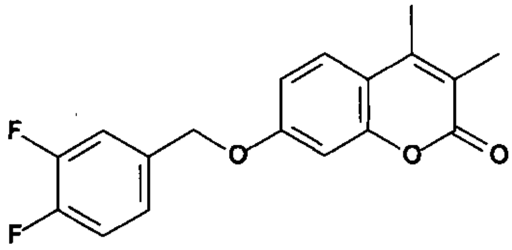

(11) Coumarin derivative

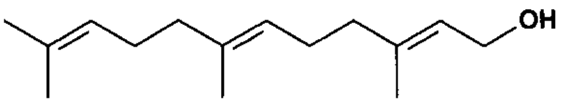

(15)*Trans,trans*-farnesol

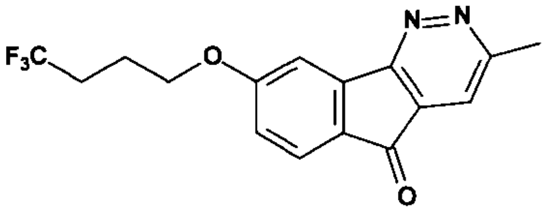

(12) 3-methyl-8-(4,4,4-trifluoro-butoxy) indenol[1,2-c]pyridazin-5-one

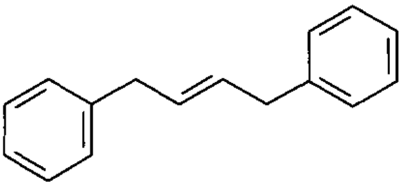

(16) 1,4-diphenyl-2-butene

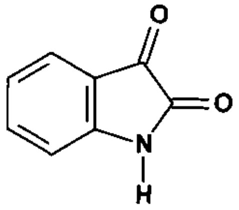

(13) Isatin

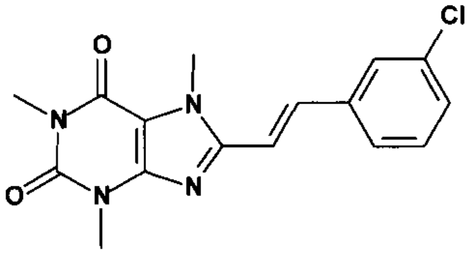

(7) CSC

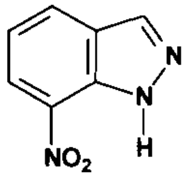

(14) 7-Nitroindazole

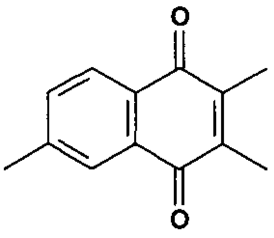

(17) TMN

Figure 3-4: The structures of previously reported reversible inhibitors of MAO-B.

A particularly potent inhibitor is structure **12** that was recently reported by Ooms *et al.*, (2002). Compound **12** was found to inhibit baboon liver MAO-B with a K_i value of 14 nM. Also of particular importance to us is CSC (**7**). CSC was found to inhibit MAO-B obtained from human, baboon and mouse liver with K_i values of 235 nM, 128 nM and 100 nM, respectively (Petzer *et al.*, 2003; Vlok *et al.*, 2006). The high inhibition potencies of larger MAO-B inhibitors are believed to be dependant upon the ability of the structures to bind simultaneously to both the entrance and active site cavities of the MAO-B enzyme. In accordance with this hypothesis, X-ray crystal structures of human MAO-B co-crystallized with *trans,trans*-farnesol (**15**) and 1,4-diphenyl-2-butene (**16**) have shown that both these inhibitors traverse the entrance and substrate cavities of MAO-B upon binding (Hubalek *et al.*, 2005). A similar dual mode of binding is probably responsible for the high affinity of potent inhibitors such as CSC (**7**), and **12** for the active site of MAO-B. Smaller structures such as isatin (**13**) and 7-nitroindazole (**14**) are only able to occupy either the entrance or substrate cavity at a time. For example X-ray crystal structures of human MAO-B complexes with isatin have shown that isatin is located in the substrate cavity of the enzyme (Hubalek *et al.*, 2005).

Table 1: The potencies of selected inhibitors of MAO-B

Compound	Mode of action	K_i^a \ IC50^b	Mitochondria
(11)	Reversible	0.00114 μM^b	Rat brain MAO-B (1)
(12)	Reversible	0.014 μM^b	Baboon liver MAO-B (2)
(13)	Reversible	3 μM^a	Human liver MAO-B (3)
(14)	Reversible	4 μM^a	Mouse brain MAO-B (4)
(15)	Reversible	0.8 μM^a	Human liver MAO-B (3)
(16)	Reversible	0.8 μM^a	Human liver MAO-B (3)
(7)	Reversible	0.128 μM^a	Baboon liver MAO-B (5)
(17)	Reversible	6 μM^a	Human liver MAO-B (6)

[1]Gnerre *et al.*, 2000; [2]Ooms *et al.*, 2003; [3]Hubálek *et al.*, 2005; [4]Castagnoli *et al.*, 1997; [5]Vlok *et al.* 2006; [6]Khalil *et al.*, 2000.

3.6 MAO-B inhibition and adenosine A$_{2A}$ receptor antagonism

The principal therapeutic agents used in the management of Parkinson's disease (PD) enhance nigrostriatal dopaminergic flux through either replenishment of depleted dopamine stores or the action of dopaminergic agonists. However, long term use of these traditional treatments can lead to loss of drug efficacy and the onset of unwanted dyskinesias (Marsden *et al.*, 1982).

Consequently alternative therapeutic strategies to treat PD that target non-dopamine systems are under development.

Adenosine is present in all mammalian tissues where it has a variety of physiological functions (Pelleg & Porter, 1990). One of these functions is to act as a neuromodulator through the interaction of G protein-coupled receptors, the adenosine receptors. Currently four adenosine receptors have been characterized and cloned, A_1, A_{2A}, A_{2B} and A_3 (Fredholm *et al.*, 1994). The intracellular signaling pathway of these receptors involves adenylate cyclase catalyzed formation of cyclicAMP. Adenosine activation of A_1 and A_3 inhibits cyclic AMP formation while interaction with A_{2A} and A_{2B} activates cyclic AMP formation (Ongini & Fredholm, 1996). In the early 1900s it became clear that the A_{2A} receptor had distinctly different properties from the other adenosine receptors (Ongini *et al.*, 2001), and has been linked most closely to dopaminergic neurotransmission and CNS motor activity (Morelli *et al.*, 1994). Antagonists of the A_{2A} receptor subtype became an attractive non-dopaminergic drug target (Xu *et al.*, 2005), in the treatment of neurological diseases, such as Parkinson's disease (Richardson *et al.*, 1997). Adenosine A_{2A} receptor antagonists for example CSC (**7**) (**Figure 3-5**) and KW-6002 (**18**) may provide symptomatic relief in PD and have displayed neuroprotective properties based on studies in the 1-methyl-4-phenyl-1,2,3,6-tetrahydropyridine (MPTP) mouse model of nigrostriatal neurodegeneration (Castagnoli *et al.*, 2003). KW-6002 has been demonstrated to increase motor activity in PD patients in a recent clinical phase IIB trial. The potential neuroprotective effect is further substantiated by the demonstration that pharmacological blockade of A_{2A} receptors by the xanthines, specific A_{2A} antagonists, or genetic depletion of the A_{2A} receptor, attenuate dopaminergic neurotoxicity and neurodegeneration in animal models of PD (Chen *et al.*, 2006).

(*E*)-8-(3-Chlorostyryl)caffeine (CSC) (**7**), the lead compound for this study, and the structurally related KW6002 (**18**) bind to the adenosine A_{2A} receptor with K_i values of 54 nM (Petzer *et al.*, 2003) and 2.2 nM (Shimada *et al.*, 1997) respectively. The dualistic properties of CSC, creates the possibility that structural analogues (**8a-f**) synthesized in this study, might possess similar activity.

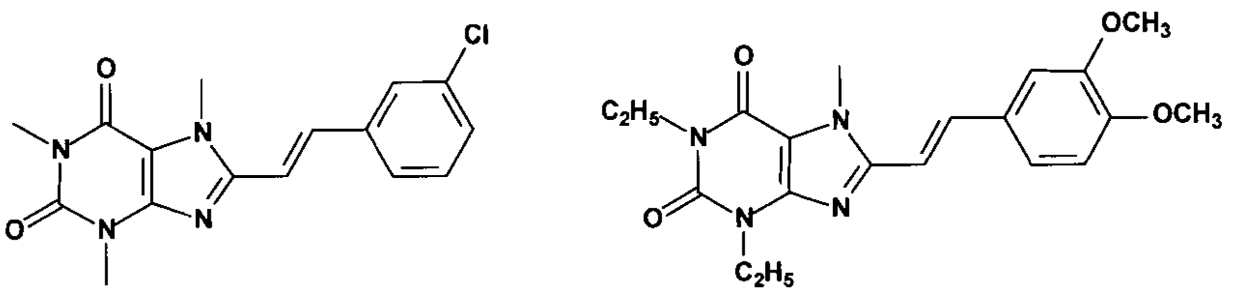

CSC (7) **KW-6002 (18)**

Figure 3-5: The structures of adenosine A_{2A} receptor antagonists CSC (**7**) and KW-6002 (**18**)

3.7 Approaches to the measurement of MAO-B activity *in vitro*

To determine the catalytic activity of the MAO-B enzyme, spectrophotometric techniques are frequently applied (Houslay *et al.*, 1974). Radiometric (Fuller *et al.*, 1970), fluorometric (Zhou *et al.*, 1996), luminometric (O'Brien *et al.*, 1993) and ammonia detection (Meyerson *et al.*, 1978) methods are less frequently used.

Because of their ease and speed of operation, our laboratory made use of spectrophotometric assays to measure MAO-B catalytic activity. Spectrophotometric detection of MMDP$^+$ (**20**), the MAO-B catalyzed oxidation product of 1-methyl-4-(1-methylpyrrol-2-yl)-1,2,3,6 tetrahydropyridine (MMTP) (**19**) (structurally related to MPTP), is measured at a wavelength of 420 nm. MMTP acts as the substrate and is oxidized to the corresponding dihydropyridinium species MMDP$^+$ (**Figure 3.6**) that is stable to further oxidation, unlike the MPTP (**1**) oxidation intermediate. MPTP is less suitable as substrate for the spectrophotometric method of analysis since oxidation of MPTP leads to an unstable intermediate (MPDP$^+$) (**20**). When MPTP is used as a substrate the HPLC method, described by Castagnoli *et al.* (1997), is used to quantify MPDP$^+$ and MPP$^+$ concentrations. MMTP is therefore the more suitable substrate (Inoue *et al.*, 1999).

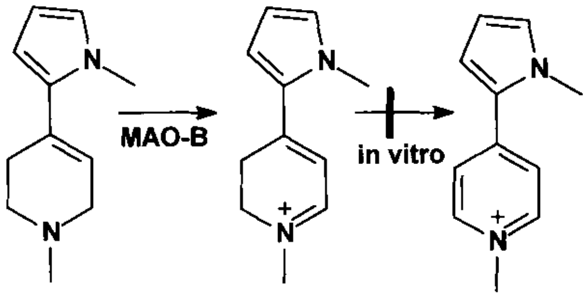

MMTP (19) **MMDP⁺(20)**

Figure 3-6: The oxidation of MMTP (**19**) to form the spectrophotometrically quantifiable MMDP$^+$ (**20**). MMDP$^+$ is stable to further oxidation *in vitro*.

For the spectrophotometric determination of MAO-B activity (with MMTP (**19**) as substrate), the measured absorbance (Abs) of the dihydropyridinium metabolite MMDP$^+$ (**20**), the reported molar extinction (ε) for MMDP$^+$ (24,000 M^{-1}) together with the enzyme concentration [E] (0.15 mg protein/mL) and incubation time (15 minutes) is substituted in equation 1 (Inoue *et al.*, 1999). The dimensions of V_i in this equation is mol.mg protein^{-1}.min^{-1} of the dihydropyridinium formed.

$$V_i = \frac{Abs}{\varepsilon} \times \frac{1}{[E]} \times \frac{1}{Time}$$ **Equation 1**

Radiometric analysis is based on the detection of the labeled MAO-B catalyzed oxidation product after incubation with a radio labeled substrate. Fuller *et al.* (1970) measured the rate of oxidation of ^{3}H-tyramine after extracting the deaminated metabolite into organic solvent. Radiometric assays are however, limited to the availability of labeled compounds. Luminometric assays are based on measurement of the light produced from peroxidase-catalyzed chemiluminescent oxidation of luminol. This is dependant on the amount of hydrogen peroxide produced in the MAO reaction (O'Brien *et al.*, 1993). This method is very sensitive and enables the analysis of substrates that produce products that are not readily detected.

Another very sensitive procedure is based on fluorometric detection. Zhou *et al.* (1996) reported that kynuramine is oxidatively deaminated and intramolecularly cyclisized to form 4-hydroxyquinoline (**Figure 3-7**). 4-Hydroxyquinoline is fluorescent and can easily be quantified in the presence of non-fluorescent substrate. Finally, assays based on the detection of ammonia are only applicable for detecting the metabolites of primary amines (Meyerson *et al.*, 1978).

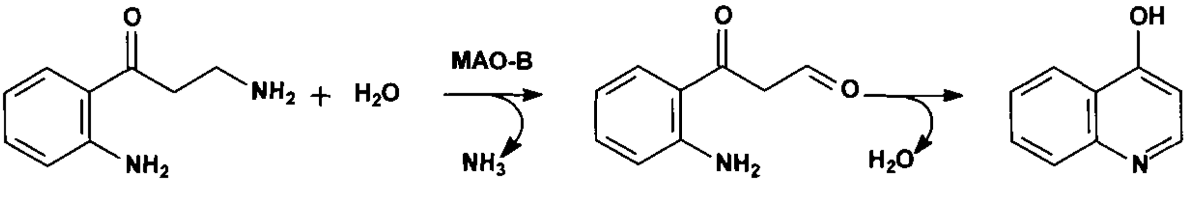

Kynuramine (21)

4-Hydroxyquinoline (22)

Figure 3-7: The oxidation of kynuramine (**21**) by MAO-B and subsequent cyclization to yield 4-hydroxyquinoline (**22**).

3.8 Enzyme kinetics – K_m and V_{max} determination

The substrate concentration that produces half maximal velocity is termed the K_m value or the Michealis constant. The constant can be determined by graphing V_i as a function of [S] (**Figure 3-8**). V_i is the measured initial velocity, when very little substrate has reacted. If the concentration of a substrate [S] is increased while al the other conditions are kept constant, V_i reaches V_{max} where the enzyme is said to be "saturated". V_{max} is almost always reached because the substrate is present in large molar excess compound to the enzyme.

When [S] is approximately equal to the K_m, V_i is very responsive to changes in [S], and the enzyme is working at half-maximal velocity. In fact many enzymes possess K_m value that approximate the physiological concentration of their substrates. The Michealis-Menten equation (**equation 2**) describes the behavior of many enzymes as the [S] is varied:

$$V_i = \frac{V_{\max} \times [S]}{K_m + [S]}$$ **Equation 2**

To determine the numeric value for V_{max}, sometimes requires impractically high concentrations of the substrate to achieve saturation. To overcome this, linear equations are used that permit ready extrapolation of V_{max} and K_m. The Michealis-menten equation (**equation 2**), is inverted and factored in order to obtain its linear form (equation 5). This equation is termed the double reciprocal or Lineweaver-Burke plot (**Figure 3-9**). V_{max} and K_m values can now easily be gathered from the graph.

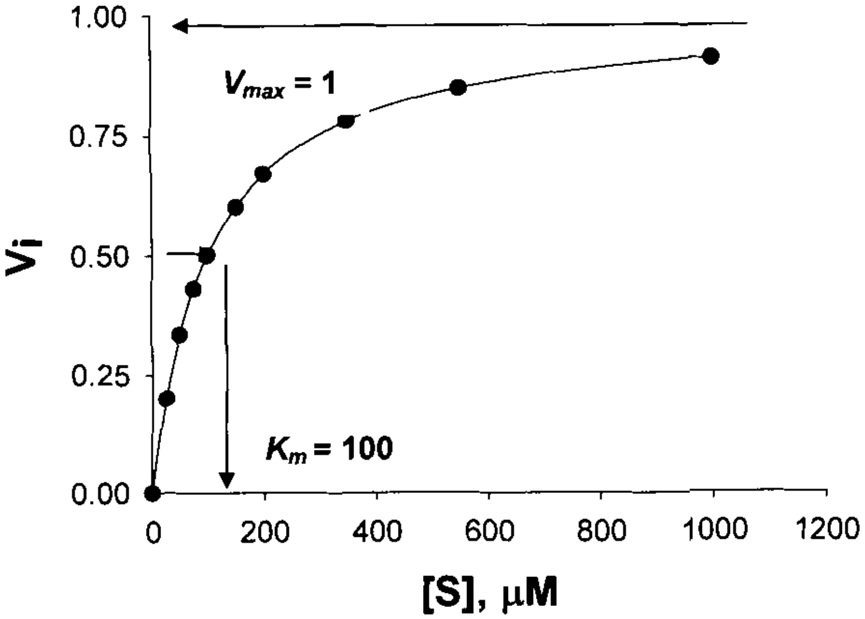

Figure 3-8: Graphical presentation of the Michealis-Menten equation (V_i versus [S])

The inverse of the Michealis-Menten equation:

$$\frac{1}{V}=\frac{K_m+[S]}{V_{\max}[S]}$$ **Equation 3**

Factor:

$$\frac{1}{V}=\frac{K_m}{V_{\max}}\times\frac{1}{[S]}+\frac{[S]}{V_{\max}[S]}$$ **Equation 4**

Simplified:

$$\frac{1}{V_i}=\frac{K_m}{V_{\max}}\times\frac{1}{[S]}+\frac{1}{V_{\max}}$$ **Equation 5**

The K_m value may be estimated from the double reciprocal or Lineweaver-Burke plot (**Figure 3-9**) using either the slope and the *y* intercept or the negative *x* intercept. Since [S] has a mathematical unit of molarity, the dimensions of K_m are moles per liter. Velocity, V_i, may be expressed in any units, since K_m is independent of enzyme concentration, [Enz]. The double-reciprocal treatment requires relatively few points to define K_m and is the method most often used to determine K_m (Murray *et* al. (2000:25).

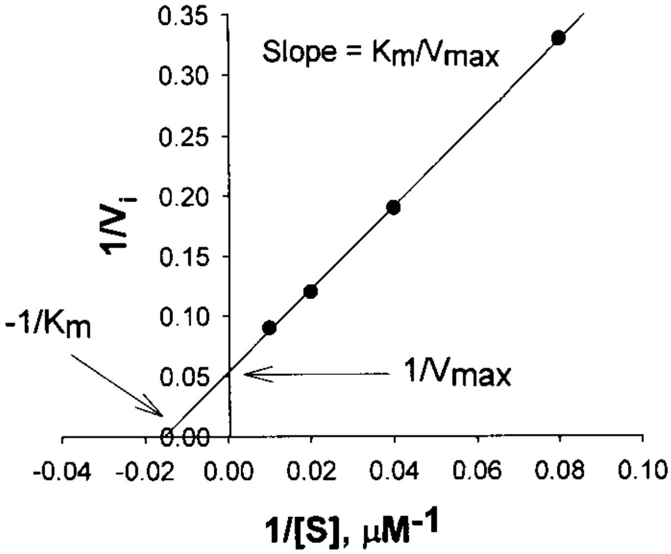

Figure 3-9: A Lineweaver-Burke plot ($1/V_i$ versus 1/[S]).

3.9 Enzyme kinetics – K_i determination

Determination of an inhibitor's K_i value, describes the affinity that the inhibitor has for the active site of the enzyme. Competitive inhibitors compete with the substrate for the same site, the catalytic site. Lineweaver-Burke plots facilitate the evaluation of competitive inhibitors. The lines drawn through the experimental points coincide at the *y* axis ($1/V_{max}$), this states that at an infinitely high concentration of S (1\[S] = 0), V_i is the same as in the absence of the inhibitor. The value of the negative of the x intercept indicates the $1/K_m$ value for substrates. Therefore addition of a competitive inhibitor increases the slope of the straight line, and therefore the apparent K_m value of the inhibitor.

Competitive inhibition occurs at the substrate binding (catalytic) site. The chemical structure of a substrate analogue inhibitor (**I**) generally resembles that of the substrate (**S**). An inhibitor-enzyme complex (**EnzI**) forms when the inhibitor binds reversibly with the enzyme. When an inhibitor and substrate are present they compete for the catalytic site of the enzyme. The action of competitive inhibitors may be understood in terms of the following reactions illustrated in **Figure 3-10**, and by **equation 6**. This equation illustrates that the K_i value is calculated by product of the unbound enzyme concentration and the unbound inhibitor concentration divided by the concentration of the enzyme-inhibitor complex.

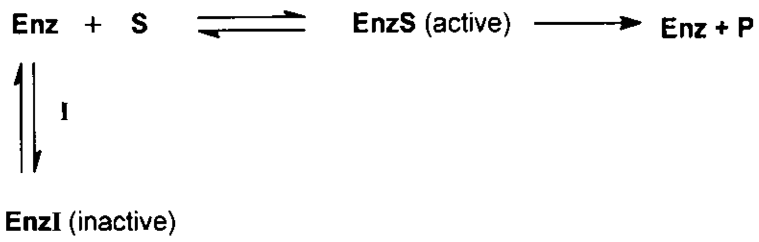

$$K_i = \frac{[Enz][I]}{[EnzI]}$$ **Equation 6**

Figure 3-10: Competitive inhibition reaction scheme.

The rate of product (**P**) formation depends solely on the concentration of the enzyme-substrate (**EnzS**) complex available. K_i values are directly proportionate to the strength of bonding between the enzyme and inhibitor if the K_i value is small, very little free enzyme (**Enz**) is available for the formation of the enzyme-substrate (**EnzS**) complex. The reaction rate will therefore be slow, and the concentration of product (**P**) little. But for an equal concentration of an inhibitor that binds less tightly (K_i = larger number) the rate of catalyzed reaction will not be decreased to such a large extent.

Double reciprocal plots facilitate evaluation of inhibitors (**Figure 3-11**). The reaction velocity (V_i) at fixed concentrations of the test inhibitor are measured against various concentrations of the substrate. The lines drawn coincide at the *y* axis. Since the y intercept is equal to V_{max}, at an infinitely high concentration of S, V_{max} in the presence and absence of the inhibitor will be equal. However, the intercept on the *x* axis, a characteristic related to the K_m value, varies with inhibitor concentration. The value at this specific interception point becomes a larger number in the presence of the inhibitor. And therefore, a competitive inhibitor raises the apparent K_m value for the substrate. Since K_m is the substrate concentration at which the concentration of the free enzyme is equal to the substrate-enzyme complex (**EnzS**), substantial free enzyme is available to react and combine with the inhibitor. K_i values for a series of competitive inhibitors indicate their effectiveness. At low concentration, those with the lowest K_i values, will be more potent inhibitors and therefore cause the greatest deal of inhibition. Many clinical drugs competitively inhibit important enzymes in microbial and animal cells (Murray *et* al. (2000:25).

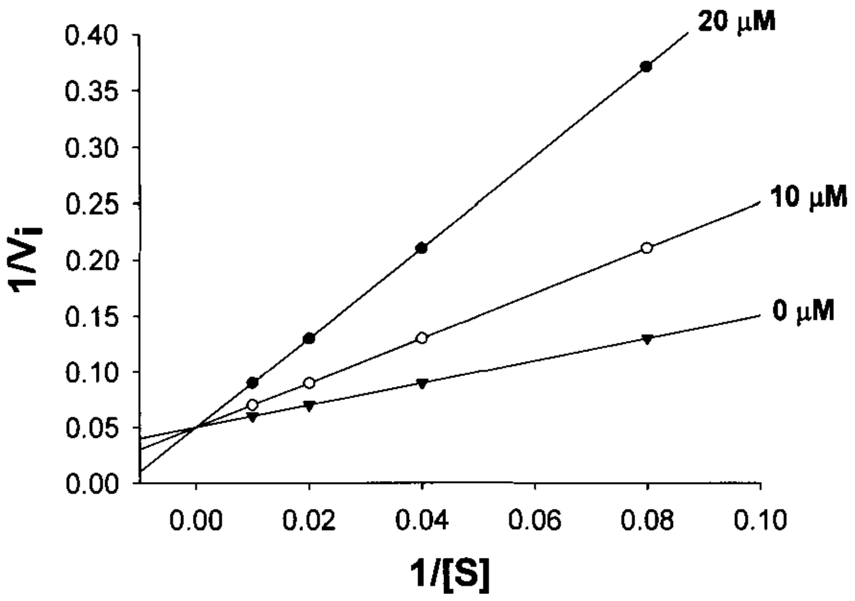

Figure 3-11: A Lineweaver-Burke plot of a reversible inhibitor with inhibitor concentrations of 0, 10 and 20 μM.

In order to determine the K_i value of a competitive inhibitor from the Lineweaver-Burk plots (**Figure 3-11**), the slopes of each plot is replotted versus the inhibitor concentration (**Figure 3-12**). The K_i value is equal to the negative on the x-axis intercept. This method is used frequently to determine the competitive K_i values.

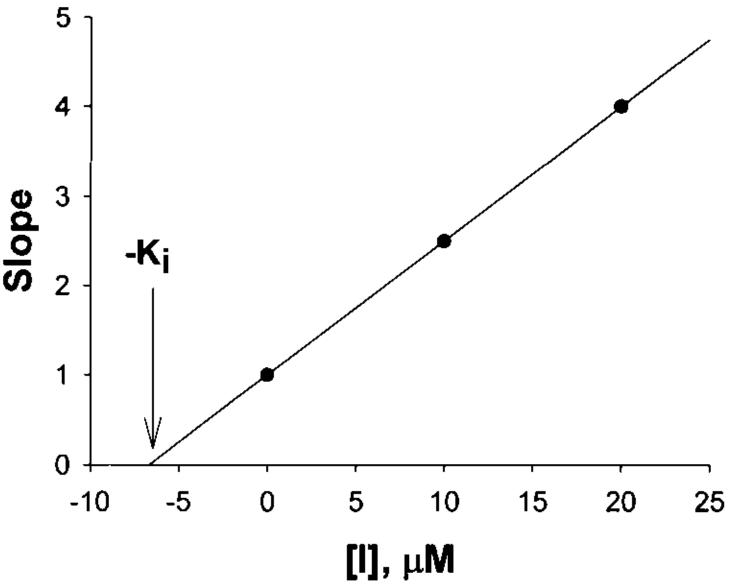

Figure 3-12: A graphical illustration of estimating a K_i value from Lineweaver-Burke plots.

3.10 Experimental Section

In the present study we have examined the possibility that the synthetic caffeine analogues (**8a–f**) may act as inhibitors of MAO-B. The measurement of MAO-B activity in our laboratory is based on the MAO-B catalyzed oxidation of 1-methyl-4-(1-methylpyrrol-2-yl)-1,2,3,6-tetrahydropyridine (MMTP) to the corresponding dihydropyridinium metabolite ($MMDP^+$) (Inoue *et al.*, 1999). Since $MMDP^+$ absorbs light maximally at a wavelength of 420 nm, the enzymatic production of $MMDP^+$ may be readily measured spectrophotometrically. At this wavelength neither the substrate nor the test inhibitors absorb light. Because of these favorable chromophoric characteristics and the *in vitro* chemical stability of $MMDP^+$ this assay is frequently used to evaluate the potencies of potential inhibitors of MAO-B (Vlok *et al.*, 2006; Petzer *et al.*, 2003). As enzyme source we have employed the mitochondrial fraction obtained from baboon liver tissue since it is reported to be devoid of MAO-A activity, while exhibiting a high degree of MAO-B catalytic activity (Inoue *et al.*, 1999). Therefore even though MMTP is a MAO-A/B mixed substrate, its oxidation by baboon liver mitochondria can be exclusively attributed to the action of the MAO-B isoform. Also the interaction of reversible inhibitors with MAO-B obtained from baboon liver tissue appears to be similar to the interaction with the human form of the enzyme since inhibitors such as CSC are equipotent with both enzyme sources (Petzer *et al.*, 2003).

3.11 MAO-B incubations for the inhibition studies

Mitochondria were isolated from baboon liver tissue as described by Salach and Weyler (1987) and stored at –70 °C in 300 µL aliquots. Following addition of a equal volume of sodium phosphate buffer (100 mM, pH 7.4) containing glycerol (50%, w/v) to the aliquots, the protein concentration was determined by the method of Bradford using bovine serum albumin as reference standard (Bradford, 1976). Since the mitochondrial fraction obtained from baboon liver tissue is reported to be devoid of MAO-A activity (Inoue *et al.*, 1999), inactivation of this enzyme was unnecessary. The MAO-A and –B mixed substrate MMTP (K_m = 60.9 µM for baboon liver MAO-B) (Inoue *et* al., 1999) served as substrate for the inhibition studies. Incubations were carried out in sodium phosphate buffer (100 mM, pH 7.4) and contained MMTP (30–120 µM), the mitochondrial isolate (0.15 mg protein/mL) and various concentrations of the test inhibitors. The final volume of the incubations was 500 µL. The stock solutions of the inhibitors were prepared in DMSO and were added to the incubation mixtures to yield a final DMSO concentration of 4% (v/v). DMSO concentrations higher than 4% are reported to inhibit MAO-B (Gnerre *et al.*, 2000). Following incubation at 37 °C for 15 min, the enzyme reactions were terminated by the addition of 10 µL perchloric acid (70%) and the samples were centrifuged at 16,000*g* for 10 minutes. The MAO-B catalyzed production of $MMDP^+$ is reported to be linear for the first 15 minutes of incubation under these conditions (Inoue *et al.*, 1999). The supernatant fractions were removed and the concentrations of the MAO-B generated product, $MMDP^+$, were measured spectrophotometrically at a wavelength of 420 nm (ε = 24,000 M^{-1}) (Inoue *et al.*, 1999). The initial rates of oxidation at four different substrate concentrations (30–120 µM) in the absence and presence of three different concentrations of the inhibitors were calculated and Lineweaver-Burke plots were constructed. The slopes of the Lineweaver-Burke plots were plotted versus the inhibitor concentration and the K_i value were determined from the x-axis intercept (intercept= $-K_i$). Linear regression analysis was performed using the Sigma Plot software package (Systat Software Inc.).

3.12 Results

All of the compounds that were evaluated (**8a-f**) in this study were found to be inhibitors of MAO-B. As demonstrated by example with (*E*)-8-(2-thienylethenyl)caffeine (**8e**) (**Figure 3-14**) and (*E*)-8-(3,5-ditrifluoromethylstyryl)caffeine (**8b**) (**Figure 3-15**), the lines of the Lineweaver–Burke plots intersected at the y-axis. This indicates that the mode of inhibition was competitive and therefore implies that the inhibitors interact reversibly with the enzyme. The K_i values for the inhibition of MAO-B by the test compounds are presented in Table 1. The most potent inhibitor was found to be (*E*)-8-(3,4-dichlorostyryl)caffeine (**8c**) with a K_i value of 36 nM. This compound was approximately 3.5 times more potent that the lead compound for this study, CSC. CSC is reported to have a K_i value of 128 nM for the inhibition of baboon liver MAO-B.

The second most potent inhibitor evaluated in this study was (*E*)-8-(3-bromostyryl)caffeine (**8a**). This inhibitor has a K_i value of 83 nM. Applying a multivariate predictive equation constructed in a previous study (Vlok *et al.*, 2006) we were able to predict the K_i value for the inhibition of MAO-B by **equation 7**. The reported σ_m and V_w values for a bromine substituted in the meta position of a phenyl ring are 0.39 and 1.32, respectively.

$$\mathrm{Log}K_i = -2.10(\pm 0.19)\sigma_m - 0.49(\pm 0.09)V_w + 0.49(\pm 0.07) \quad \textbf{Equation 7}$$

Substitution of these values into the multivariate equation above yield a predicted K_i value of 106 nM. The small difference between the experimentally obtained K_i value of 83 nM and the predicted value may be considered proof of the validity of the equation.

Another inhibitor identified in this study as an exceptionally potent inhibitor is (*E*)-8-(3,5-ditrifluoromethylstyryl)caffeine (**8b**). This compound was found to inhibit MAO-B with a K_i value of 239 nM. (*E*)-8-(2-Thienylethenyl)caffeine (**8e**), (*E*)-8-(3-thienylethenyl)caffeine (**8f**) and (*E*)-8-(2-furylethenyl)caffeine (**8d**) were found to be only moderate inhibitors of MAO-B with K_i values in the low micro molar range. Although less potent than the other inhibitors evaluated in this study (*E*)-8-(2-thienylethenyl)caffeine (**8e**) was still a better inhibitor than (*E*)-8-styrylcaffeine. (*E*)-8-styrylcaffeine has a reported K_i value for the inhibition of baboon liver mitochondria of 3 µM (Vlok *et al.*, 2006).

Table 2: The K_i values for the inhibition of MAO-B by (*E*)-8-styrylcaffeine analogues (**8a–f**).

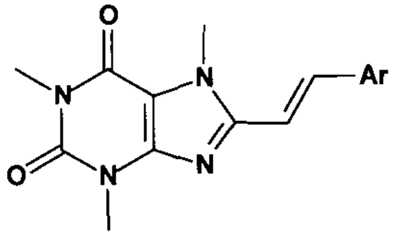

	Ar	K_i (µM)		Ar	K_i (µM)
8a	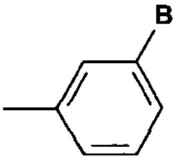	0.083	**8d**	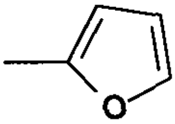	39.7
8b	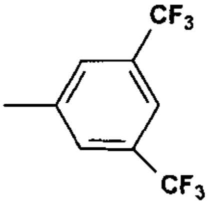	0.239	**8e**	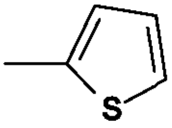	1.58
8c	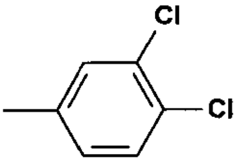	0.036	**8f**	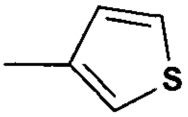	11.3

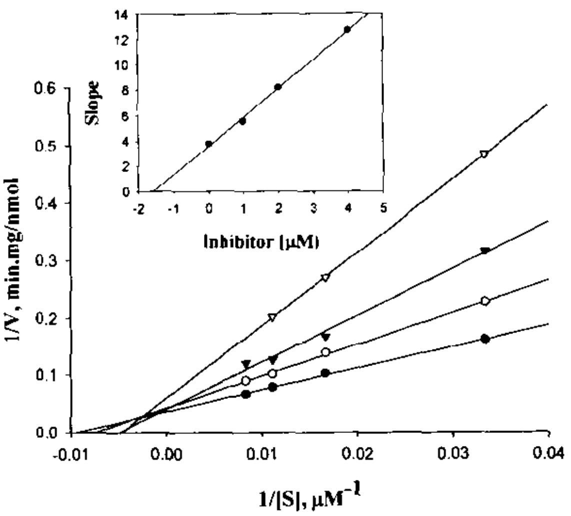

Figure 3-13: Lineweaver–Burke plots of the oxidation of MMTP by baboon liver MAO-B in the absence (filled circles) and presence of various concentrations of **8e** (open circles, 1 μM; filled triangles, 2 μM; open triangles, 4 μM). The concentration of the baboon liver mitochondrial preparation was 0.15 mg/mL and the rates are expressed as nmoles.mg protein^{-1}.min^{-1} of MMDP$^+$ formed. The inset is the replot of the slopes versus the inhibitor concentrations.

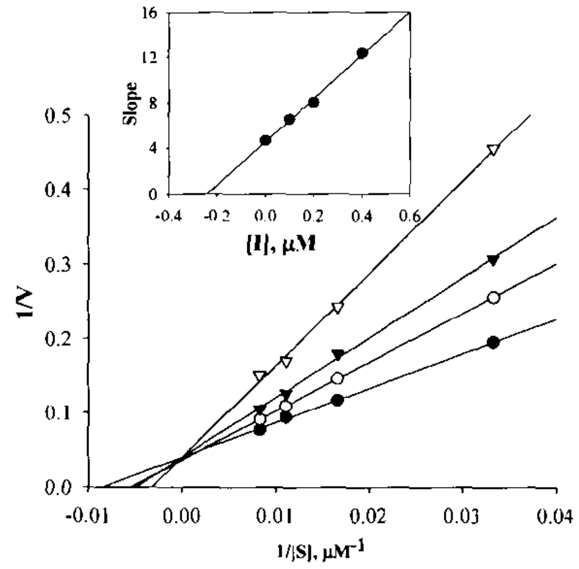

Figure 3-14: Lineweaver–Burke plots of the oxidation of MMTP by baboon liver MAO-B in the absence (filled circles) and presence of various concentrations of **8b** (open circles, 0.1 μM; filled triangles, 0.2 μM; open triangles, 0.4 μM). The concentration of the baboon liver mitochondrial preparation was 0.15 mg/mL and the rates are expressed as nmoles.mg protein^{-1}.min^{-1} of MMDP$^+$ formed. The inset is the replot of the slopes versus the inhibitor concentrations.

3.13 Conclusion

All of the compounds that were evaluated (**8a-f**) in this study were found to be inhibitors of MAO-B. The mode of inhibition was found to be competitive and therefore the inhibitors interact reversibly with the enzyme. The most potent inhibitor was found to be (*E*)-8-(3,4-dichlorostyryl)caffeine (**8c**) with a K_i value of 36 nM. This compound was approximately 3.5 times more potent that the lead compound for this study, CSC. CSC is reported to have a K_i value of 128 nM for the inhibition of baboon liver MAO-B.

The second most potent inhibitor evaluated in this study was (*E*)-8-(3-bromostyryl)caffeine (**8d**). This inhibitor has a K_i value of 83 nM. The small difference between the experimentally obtained K_i value of 83 nM and the predicted value of 106 nM may be considered proof of the validity of the predictive equation.

Another inhibitor identified in this study as an exceptionally potent inhibitors is (*E*)-8-(3,5-ditrifluoromethylstyryl)caffeine. This compound was found to inhibit MAO-B with a K_i value of 239 nM. (*E*)-8-(2-Thienylethenyl)caffeine (**8e**), (*E*)-8-(3-thienylethenyl)caffeine (**8f**) and (*E*)-8-(2-furylethenyl)caffeine (**8d**) were found to be only moderate inhibitors of MAO-B with K_i values in the low micro molar range. Although less potent than the other inhibitors evaluated in this study (*E*)-8-(2-thienylethenyl)caffeine (**8e**) was still a better inhibitor than (*E*)-8-styrylcaffeine. (*E*)-8-styrylcaffeine has a reported K_i value for the inhibition of baboon liver mitochondria of 3 µM. (Vlok *et al.*, 2006). These results suggest that electron deficiency of the styryl ring is not the only requirement for (*E*)-8-styrylcaffeine analogues to act as potent inhibitors of MAO-B. Hydrophobic interactions between styryl substituents and active site residues may play an important role in stabilizing the enzyme-inhibitor complex. The lack of such substituents in compounds **8d-f** may explain their relatively lower inhibition potencies compared to the other structures examined in this study. This argument is further supported by the finding that (*E*)-8-(3-bromostyryl)caffeine (**8d**) is a more potent inhibitor than CSC even though bromine is less electron-withdrawing than chlorine.

Conclusion

Chapter

4

4.1 Conclusion and Summary

The crystal structures of human recombinant MAO-B in complex with several pharmacological important inhibitors of the enzyme have recently been reported (Binda *et al.*, 2004; Binda *et al.*, 2003; Hubalek *et al.*, 2005). From the surface of the enzyme, the access channel leading to the active site FAD co-factor consists of an entrance followed by a substrate cavity. An inhibitor must transverse an entrance cavity in order to gain access to the substrate cavity. This is true for small molecule inhibitors such as isatin that has been shown to bind within the substrate cavity of the enzyme (Binda *et al.*, 2003). A larger inhibitor such as the reversible inhibitor 1,4-diphenyl-2-butene (**16**) (**Figure 3-4**) appears to exhibit a dual binding mode that involves traversing both the entrance and substrate cavities (Binda *et al.*, 2003).

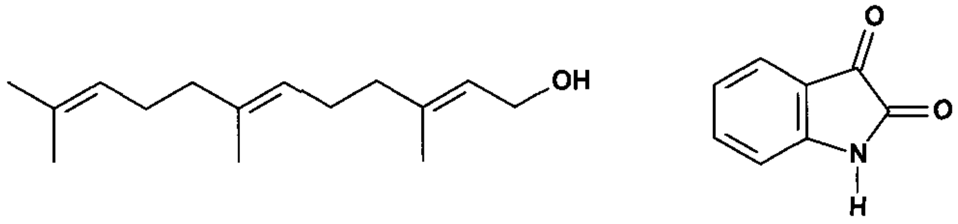

(15)*Trans,trans*-farnesol **(13) Isatin**

Figure 4-1: Structures of *trans,trans-farnesol* (**15**) and isatin (**13**).

Another inhibitor, *trans,trans*-farnesol (**15**) is also reported to span both the entrance and substrate cavities with the polar OH moiety in close contact with the flavin located in the substrate cavity (Hubalek *et al.*, 2005). The gate separating the two cavities is the side chain of Ile-199 which is thought to exhibit different rotamer conformations that allows for the fusion of the two cavities in order to accommodate these larger inhibitors (Binda *et al.*, 2003). The potency of MAO-B inhibition by (*E*)-8-styrylcaffeines may possibly also be explained by a similar mode of binding that involves traversing both the entrance and substrate cavities (Binda *et al.*, 2006). These inhibitors possibly bind to MAO-B with the caffeine ring located in the substrate cavity of the active site while the styryl substituent extends into the entrance cavity. In support of this hypothesis caffeine was reported to be a very weak inhibitor of MAO-B (Chen *et al.*, 2001). Without the styryl side chain, caffeine is expected to bind to either the substrate or the entrance cavity leaving the other cavity unoccupied. Therefore styryl substitution possibly assists with dual binding that may lead to increased inhibition potency.

The important role played by the styryl side chain is further supported by the observation that substitution of the phenyl ring has a considerable effect on the potency by which (E)-8-styrylcaffeine analogues inhibit MAO-B. Since the styryl ring of these inhibitors is thought to bind within the entrance cavity, specific interactions between the styryl substituents and amino acid side chains in the entrance cavity may explain these observations. It may be predicted that bulky and lipophylic styryl substituents may lead to increased binding affinity since the entrance cavity is lined by the side chains of hydrophobic amino acids (Binda et al., 2002). In accordance with this expectation, we have previously found that for (E)-8-styrylcaffeine analogues bearing different substituents at C-4 of the styryl ring (Vlok et al., 2006), the potency of MAO-B inhibition correlated with both the size (Vw) and the lipophylicity (π) of the substituents. Enhancement of the size and lipophylicity of the substituents resulted in better inhibition. In the present study it was demonstrated that relative large and lipophylic styryl substituents (3-Br, 3,4-di-Cl and 3,5-di-CF_3) enhanced inhibition potency to a large degree compared to the unsubstituted (E)-8-styrylcaffeine (Ki value of 2.7 µM). This suggests that these inhibitors also spans both the entrance and substrate cavities and the styryl substituents are involved in hydrophobic interactions, possibly within the entrance cavity where the styryl phenyl ring is expected to be located. The electron-deficiency of the styryl ring appears to be of lesser importance since compounds **8d**-**f** were found to be only moderate inhibitors.

Another interesting outcome of this study was that the (*E*)-8-styrylcaffeine analogue disubstituted with chlorine at C-3 and C-4 of the styryl ring (**8c**) was found to be a more potent inhibitor (K_i = 36 nM) than CSC, which is monosubstituted with chlorine at C-3 (K_i = 128 nM). We have previously reported that the (*E*)-8-styrylcaffeine analogue that is monosubstituted with chlorine at C-4 (K_i = 260 nM) also inhibits MAO-B potently (Vlok et al., 2006). This synergistic effect of disubstitution on MAO-B inhibition suggests that there exists, possibly within the entrance cavity, an aromatic binding pocket with at least two major interaction sites, one for substituents at C-3 of the aromatic ring and another for substituents at C-4. Alternatively, the addition of a second substituent may simply enhance the lipophilicity of the inhibitor and therefore its affinity for the enzyme. We have previously shown that the lipophilicity of the C-4 styryl substituents correlates with MAO-B inhibition potency of (*E*)-8-styrylcaffeines (Vlok et al., 2006).

References

BACH, A.W.J., LAN, N.C., JOHNSON, D.L., ABELL, C.W., BEMBENEK, M.E., KWAN, S.W., SEEBURG, P.H. & SHIH, J.C. 1988. cDNA cloning of the human liver monoamine oxidase A and B: molecular basis of differences in enzymatic properties. *Proceedings of the national academy of sciences of the United States of America*, 85:4934-4938.

BINDA, C., HUBALEK, F., LI, M., CASTAGNOLI, N., EDMONDSON, D.E., MATTEVI, A. 2006. Structure of the human mitochondrial monoamine oxidase B. New chemical implications for neuroprotectant drug design. *Neurology,* 67 (7 suppl 2): S5- S7

BINDA, C., HUBALEK, F., LI, M., HERZIG, Y., STERLING, J., EDMONDSON, D.E. & MATTEVI, A. 2004. Crystal structures of monoamine oxidase B in complex with four inhibitors of the N-propargylaminoindan class. *Journal of medicinal chemistry, 47:1767-1774.*

BINDA, C., LI, M., HUBALEK, F., RESTELLI, N., EDMONDSON, D.E., MATTEVI, A. 2003. Insights into the mode of inhibition of human mitochondrial monoamine oxidase B from high resolution crystal structures. *Proceedings of the national academy of sciences of the United States of America*, 100:9750-9755.

BLICKE, F.F. & GODT, H.C., JR. 1954. Reactions of 1,3-dimethyl-5,6-diaminouracil. *Journal of the American chemical society*, 76:2798-2800.

BONNEH-BARKAY, D., ZIV, N., & FINBERG, J.P. 2005. Characterization of the neuroprotective activity of rasagiline in cerebellar granule cells. *Neuropharmacology, 48:406-416.*

BRADFORD, M.M. 1976. A rapid and sensitive method for the quantitation of microgram quantities of protein utilizing the principle of protein-dye binding. *Analytical biochemistry*, 72:247-254.

CASTAGNOLI, K., PALMER, S., ANDERSON, A., BUETERS, T. & CASTAGNOLI, N., JR. 1997. The neuronal nitric oxide synthase inhibitor 7-nitroindazole also inhibits the monoamine oxidase-B-catalyzed oxidation of 1-methyl-4-phenyl-1,2,3,6-tetrahydropyridine. *Chemical research in toxicology*, 14:523-527.

CASTAGNOLI, K., PETZER, J.P., STEYN, S.J., VAN DER SCHYF, C.J., CASTAGNOLI, N. & JR. 2003. Inhibition of human MAO-A and MAO-B by a compound isolated from flue-cured tobacco leaves and its neuroprotective properties in the MPTP mouse model of neurodegeneration. *Inflammopharmacology*, 11:183-188.

CHAZOT, P.L. 2001. Safinamide (Newton Pharmaceuticals). *Current opinion in investigational drugs*, 2:809-813.

CHEN, J.F., STEYN, S., STAAL, R., PETZER, J.P., XU, K., VAN DER SCHYFF C.J., CASTAGNOLI, K., SONSELLA, P.K., CASTAGNOLI, N. JR., SCHWATZSCHILD, M.A. 2002. 8-(3-Chlorostyryl)caffeine may attenuate MPTP neurotoxicity through dual actions of monoamine oxidase inhibition and A_{2A} receptor antagonism. *The journal of biological chemistry*, 277:36040-36044.

CHIBA, K., PETERSON, L.A., CASTAGNOLI, K.P., TREVOR, A.J. & CASTAGNOLI, N., JR. 1985. Studies on the molecular mechanism of bioactivation of the selective nigrostriatal toxin 1-methyl-4-phenyl-1,2,3,6-tetrahydropyridine (MPTP). *Drug metabolism and disposition*, 13:342-347.

CHIBA, K., TREVOR, A.J. & CASTAGNOLI, N., JR. 1984. Metabolism of the neurotoxic tertiary amine, MPTP, by brain monoamine oxidase. *Biochemical and biophysical research communications*, 120:574-578.

CHIBA, K., TREVOR, A.J. & CASTAGNOLI, N., JR. 1985. Active uptake of MPP^+, a metabolite of MPTP, by brain synaptosomes. *Biochemical and biophysical research communications*, 120:574-578.

DEL GIUDICE, M.R., BORIONI, S., MUSTAZZA, C., GATTA, F., DIONISOTTI, S., ZOCCHI, E. & ONGINI, E. 1996. (E)-1-(Heterocyclyl or cyclohexyl)-2-[1,3,7-trisubstituted(xanthin-8-yl)]ethenes as A_{2A} adenosine receptor antagonists. *European journal of medicinal chemistry*, 31:59-63.

EBADI, M., GOVITRAPONG, P., SHARMA, S., MURALIKRISHNAN, D., SHAVALI, S., PELLETT, L., SCHAFER, R., ALBANO, C. & EKEN, J. 2001. Ubiquinone (coenzyme q10) and mitochondria in oxidative stress of Parkinson's disease. *Biological signals and receptors*, 10:224-253.

EDMONDSON, D.E., MATTEVI, A., BINDA, C., LI, M., HUBALEK, F. 2004. Structure and mechanism of monoamine oxidase. *Current Medicinal Chemistry*, 11:1983-93.

FREDHOLM, B.B., ABBRACCHIN, M.P., BURNSTOCK, G., DALY, J.W., HARDEN, T.K., JACOBSON, K.A., LEFF, P. & WILLIAMS, M. 1994. Nomenclature a classification of purinoceptors. *Pharmacology reviews*, 46:143-156.

FULLER, R.W., WARREN, B.J. & MOLLOY, B.B. 1970. Selective inhibition of monoamine oxidase in rat brain mitochondria. *Biochemical pharmacology*, 19:2934-2936.

GEHA, R.M., REBRIN, I., CHEN, K., SHIH, J.C. 2001. Substrate and inhibitor specificities for the human monoamine oxidase A and B are influenced by a single amino acid. *The journal of biological chemistry*, 276: 9877-9882.

GERLACH, M., BEN-SHACHAR, D., RIEDERER, P. & YOUDIM, M.B. 1994. Altered brain metabolism of iron as a cause of neurodegenerative diseases? *Journal of neurochemistry*, 63:793-807.

GNERRE, C., CATTO, M., LEONETTI, F., WEBER, P., CARRUPT, P.A., ALTOMARE, C., CAROTTI, A. & TESTA, B. 2000. Inhibition of monoamine oxidases by functionalized coumarin derivatives: biological activities, QSARs, and 3D-QSARs. *Journal of medicinal chemistry*, 43:4747-4758.

GRIMSBY, J.N.C., NEVE, R., CHEN, K. & SHIH, J.C. 1990. Tissue distribution of human monoamine oxidase A and B mRNA. *Journal of neurochemistry*, 55:1166-1169.

HEIKKILA, R.E., HESS, A. & DUVOISIN, R.C. 1984. Dopaminergic neurotoxicity of 1-methyl-4-phenyl-1,2,5,6-tetrahydropyridine in mice. *Science*, 224:1451-1453.

HEINONEN, E.H., RINNE, U.K., TUOMINEN, J. 1989. Selegiline in the treatment of daily fluctuations in disability of parkinsonian patients with long-term L-dopa treatment. *Acta neurologica Scandanavica Suppl*, 126:113-118.

HOUSLAY, M.D., GARRET, N.J. & TIPTON, K.F. 1974. Mixed substrate experiments with human brain monoamine oxidase. *Biochemical pharmacology*, 23:1937-1944.

HUBÁLEK, F., BINDA, C., KHALIL, A., LI, M., MATTEVI, A., CASTAGNOLI, N. & EDMONDSON, D.E. 2005. Demonstration of isoleucine 199 as a structural determinant for the selective inhibition of human monoamine oxidase B by specific reversible inhibitors. *Journal of biological chemistry*, 280:15761-15766.

INOUE, H., CASTAGNOLI, K., VAN DER SCHYFF, C., MABIC, S., IGARASHI, K. & CASTAGNOLI, N. JR. 1999. Species dependant differences in the monoamine oxidase A and B catalyzed oxidation of various C-4 substituted 1-methyl-4-phenyl-1,2,3,6-tetrahydropyridinyl derivatives. *Journal of pharmacology and experimental therapeutics*, 291:856-864.

JACOBSON, K.A., GALLO-RODRIGUEZ, C., MELMAN, N., FISCHER, B., MAILLARD, M., VAN BERGEN, A., VAN GALEN, P.J.M. & KARTON, Y. 1993. Structure-activity realtionships of 8-styrylxanthines as A_2 selective adenosine antagonists. *Journal of medicinal chemistry*, 36:1333-1342.

KHALIL, A.A., STEYN, S. & CASTAGNOLI, N JR. 2000. Isolation and characterization of a monoamine oxidase inhibitor from tobacco leaves. *Chemical research in toxicology*, 13:31-35.

KUPSCH, A., SAUTTER, J., GOTZ, M.E., BREITHAUPT, W., SCHWARZ,J., YOUDIM, M.B., RIEDERER, P., GERLACH, M. & OERTEL, W.H. 2001. Monoamine oxidase-inhibition and MPTP-induced neurotoxicity in the non-human primate: comparison of rasagiline (TVP 1012) with selegiline. *Journal of neural transmission*, 108:985-1009.

MARSDEN, C.D., PERKES, J.D., QUINN, N. 1982. Fluctuations in disability in Parkinson's disease: clinical aspects. In: MARSDEN, C.D. & FAHN, S. *Movement disorders, Butterworth*

Scientific, New York. P96-122.

MEYERSON, L.A., MCMURTREY, K.D. & DAVIS, V.E. 1978. A rapid and sensitive potentiometric assay for monoamine oxidase using an ammonia-selective electrode. *Analytical biochemistry,* 86:287-297.

MORELLI, M., FENU, S., PINNA, A. & DI CHIARA, G. 1994. Adenosine A_{2A} receptors interact negatively with dopamine D1 and D2 receptors in unilaterally 6-hydroxydopamine-lesioned rats. *European journal of pharmacology,* 251:21-25.

MÜLLER, C.E., GEIS, U., HIPP, J., SCHOBERT, U., FROBENIUS, W., PAWLOWSKI, M., SUZUKI, F. & SANDOVAL-RAMIREZ, J. 1997. Synthesis and structure-activity relationships of 3,7-dimethyl-propargielxanthine derivatives, A_{2A}-selective adenosine receptor antagonists. *Journal of medicinal chemistry,* 40:4396-4405.

MURRAY, R.K., GRANNER, D.K., MAYES, P.A. & RODWELL, V.W. 2000. Harper's biochemistry. Connecticut: Stamford. 94-100 p.

NAGATSU, T. 2004. Progress in monoamine oxidase (MAO) research in relation to genetic engineering. *Neurotoxicology,* 25:11-20.

NYHOLM, D. 2006. Pharmacokinetic optimisation in the treatment of Parkinson's disease : an update. *Clinical pharmacokinetics,* 45:109-136.

O'BRIEN, E.M., KIELY, K.A. & TIPTON, K.F. 1993. A discontinuous luminometric assay for monoamine oxidase. *Biochemical pharmacology,* 46:1301-1306.

ONGINI, E. & FREDHOLM, B.B. 1996. Pharmacology of adenosine A_{2A}-receptors. *TiPS,* 17: 364-372.

ONGINI, E., MONOPOLY, A., CACCIARI, B. & BARALDI, P.G. 2001. Selective adenosine A_{2A}-receptor antagonists. *Il farmaco,* 56:87-90.

OOMS, F., FREDERICK, R. & DURANT, F. 2003. Rational approaches towards reversible inhibition of type B monoamine oxidase. Design and evaluation of a novel 5H-Indeno[1,2-c]pyridazin-5-one derivative. *Bioorganic and medicinal chemistry letters,* 13:69-73.

PALFI, M., SZOKO, E. & KALMAN, M. 2006. Molecular mechanisms of the neuroprotective effect of (-)-deprenyl. *Orvosi Hetilap,* 147:1251-1257.

PAPESCH, V. & SCHROEDER, E.F. 1951. Synthesis of 1-mono and 1,3-disubstituted 6-aminouracils. Diuretic activity. *Journal of organic chemistry*, 16:1879-1890.

PELLEG, A. & PORTER, R.S. 1990. The pharmacology of adenosine. *Pharmacotherapy*, 10:157-174.

PETZER, J.P., STEYN, S., CASTAGNOLI, K.P., CHEN, J.F., SCHWARZSCHILD, M.A., VAN DER SCHYF, C.J., CASTAGNOLI, N. 2003. Inhibition of monoamine oxidase B by selective adenosine A_{2A} receptor antagonists. *Bioorganic medicinal chemistry*, 11:1299-1310.

RABEY, J. M., SAGI, L., HUBERMAN, M., MELAMED, E., KORYZEN, A., GILADI, M., INZELBERG, R., DJALDETTI, R., KLEIN, C. & AND BERECZ, G. 2000. Rasagiline mesylate, a new MAO-B inhibitor for the treatment of Parkinson's disease: a double blind study as adjunctive therapy to L-dopa. *Clinical neuropharmacology*, 23:324-330.

RICHARDSON, P.J., KASE, H. & JENNER, P.G. 1997. Adenosine A_{2A} receptor antagonists as new agents for the treatment of Parkinson's disease. *Trends in pharmacological sciences*, 18:338-344.

SALACH, J. & WEYLER, J. 1987. Preparation of the flavin-containing aromatic amineoxidase of human placenta and beef liver. *Methods of enzymology*, 142:627-637.

SCHMIDT, N. & FERGER, B. 2001. Neurochemical findings in the MPTP model of Parkinson's disease. *Journal of neural transmission, 108: 1263-1282.*

SCHWARTZSCHILD, M.A., AGNATI, L., FUXE, K., CHEN, J.F., & MORELLI, M. 2006. Targeting adenosine A_{2A} receptors in Parkinson's disease. *Trends in neuroscience*, 29:647-654.

SHIMADA, J., KOIKE, N., NONAKA, H., SHIOZAKI, S., YANAGAWA, K., KANADA, T., KOBAYASHI, H. & FUMIO, S. 1997. Adenosine A_{2A} antagonists with potent anti-cataleptic activity. *Bioorganic and medicinal chemistry letters*, 7:2349-2352.

SHIMADA, J., SUZUKI., NONAKA, H. & ISHII, A. 1992. 8-Polycycloalkyl-1,3-dipropylxanthines as potent and selective antagonists for A1-adenosine receptors. *Journal of medicinal chemistry*, 35:924-930.

SPEER, J.H. & RAYMOND, A.L. 1953. Some alkyl homologues of theophyline. *Journal of the American chemical society*, 75:114-115.

STERLING, J., VEINBERG, A., LERNER. D., GOLDENBERG, W., LEVY, R., YOUDIM, M., FINBERG, J. 1998. *Journal of neural transmission*, 52:301-305.

SUZUKI, F., SHIMADA, J., SHIOZAKI, S, ICHIKAWA, S., ISHII, A., NAKAMURA, J., NONAKA, H., KOBAYASHI, H. & AND FUSE, E. 1993. Adenosine A1 antagonists. 3. Structure relationships on ameliorating against scopolamine- or N6-(R)-phenylisopropyl)adenosine induced cognitive disturbance. *Journal of medicinal chemistry*, 36:2508-2518.

TAKEDA, M., LI, Z.K. & HATTORI, T. 1990. Astroglial ablation prevents MPTP-induced nigrostriatal neuronal death. *Brain research*, 509:55-61.

THE PARKINSON STUDY GROUP. 1989. Effect of deprenyl on the progression of disability in early Parkinson's disease. *New England journal of medicine*, 321:1364-1371.

TRAUBE, W. 1900. Der synthetische aufbau der harnsaure, des xanthines, theobromins, theophyllins und caffeins aus der cyanessigsaure. *Chemische berigte*, 33:3035-3056.

TRIPLETT, J.W., MACK, S. W., SMITH, S.L. & DIGENIS, G.A. 1978. Synthesis of carbon-13 labeled uracil, 6,7-dimethyllumazine, and lumichrome, via commen intermediate: cyanoacetylurea. *Journal of labeled compounds and radiopharmaceuticals*, 14:35-41.

VLOK, N., MALAN, S.F., CASTAGNOLI, N., JR., BERGH, J.J. & PETZER, J.P. 2006. Inhibition of monoamine oxidase B by analogues of the adenosine A_{2A} receptor antagonist (*E*)-8-(3-chlorostyryl)caffeine (CSC). *Bioorganic medicinal chemistry*, 14:3512-3521.

VOLZ, H. P. & GLEITER, C. H. 1998. Monoamine oxidase inhibitors: a perspective on their use in the elderly. *Drugs in the aging*, 13: 341-355.

WALDEMIER, P. C. 1987. Amine oxidases and their endogenous substrates. *Journal of neural transmission*, 23 (suppl.):55-72.

XU, K., BASTIA, E. & SCHWARZSCHILD, M. 2005. Therapeutic potential of adenosine A_{2A} receptor antagonists in Parkinson's disease. *Pharmacology and therapeutics*, 105:267-310.

YOUDIM, M.B. & BAKHLE, Y.S. 2006. Monoamine oxidase: Isoforms and inhibitors in Parkinson's disease and depressive illness. *British journal of pharmacology*, 147 (suppl 1): S287-S296.

YOUDIM, M.B., BAR, A.O., YOGEV-FALACH, M., WEINREB, O., MARUYAMA, W., NAOI, M.,

&. AMIT, T. 2005. Rasagiline: neurodegeneration, neuroprotection, and mitochondrial permeability transition. *Journal of neuroscience research*, 79:172-79.

ZHOU, J.P.P, ZHONG, B. & SILVERMAN, R.B. 1996. Direct continuous fluorometric assay for monoamine oxidase. *Analytical biochemistry*, 234:9-12.

ZOCCARATO, F.; TOSCANO, P.; ALEXANDRE, A. 2005. Dopamine-derived dopaminochrome promotes H_2O_2 release at mitochondrial complex I: stimulation by rotenone, control by Ca(2+), and relevance to Parkinson disease. *Journal of biological chemistry* 280:15587-15594.

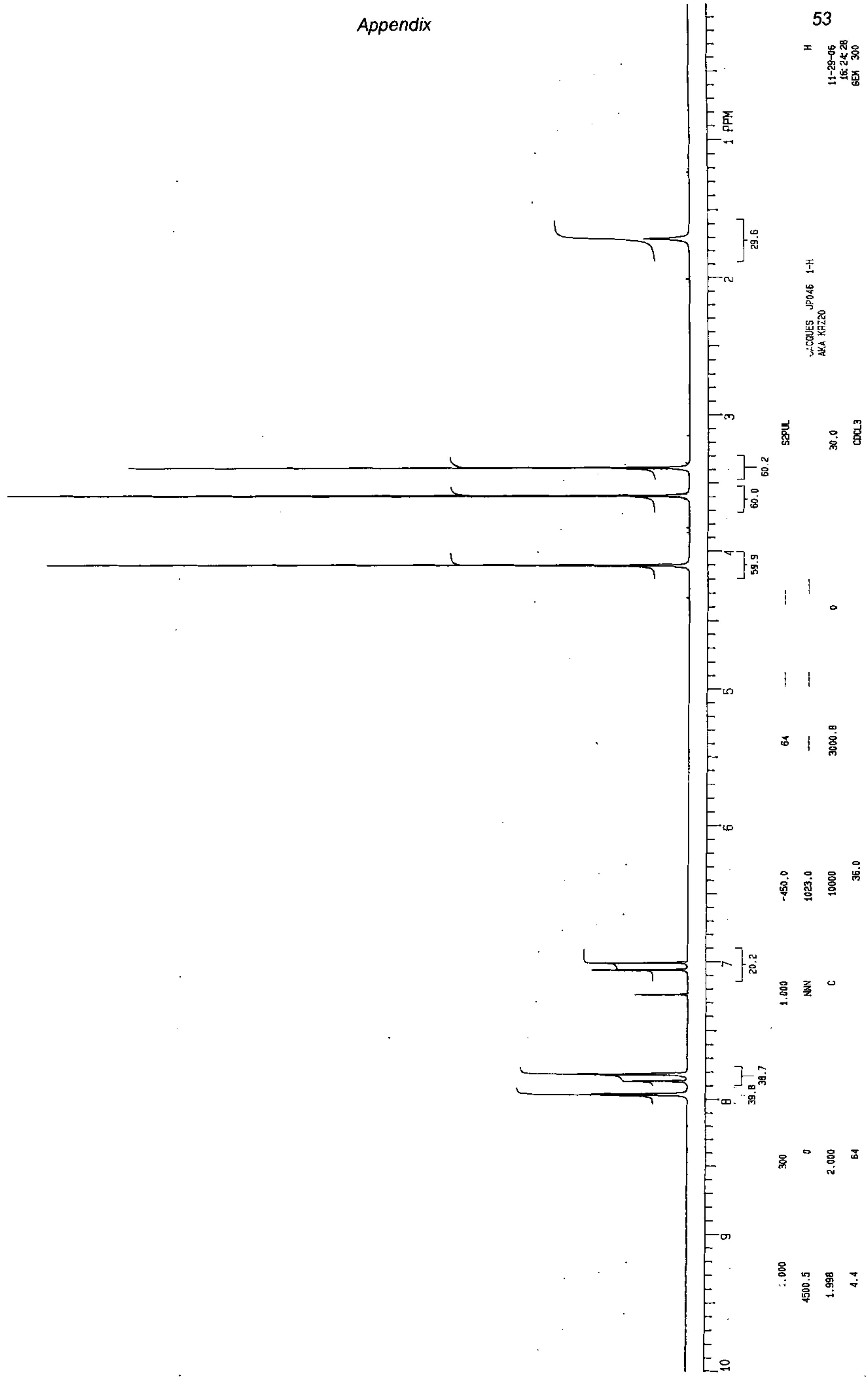
H
11-29-06
16:24:28
GEM 300
JACQUES JP046 1-H
AKA KRZ20
S2PUL
30.0
CDCL3
PPM
1
2
3
4
5
6
7
8
9
10
29.6
60.2
60.0
59.9
20.2
38.7
39.8
64
3000.8
-450.0
1023.0
10000
36.0
1.000
NNN
C
300
0
2.000
64
1.000
4500.5
1.998
4.4

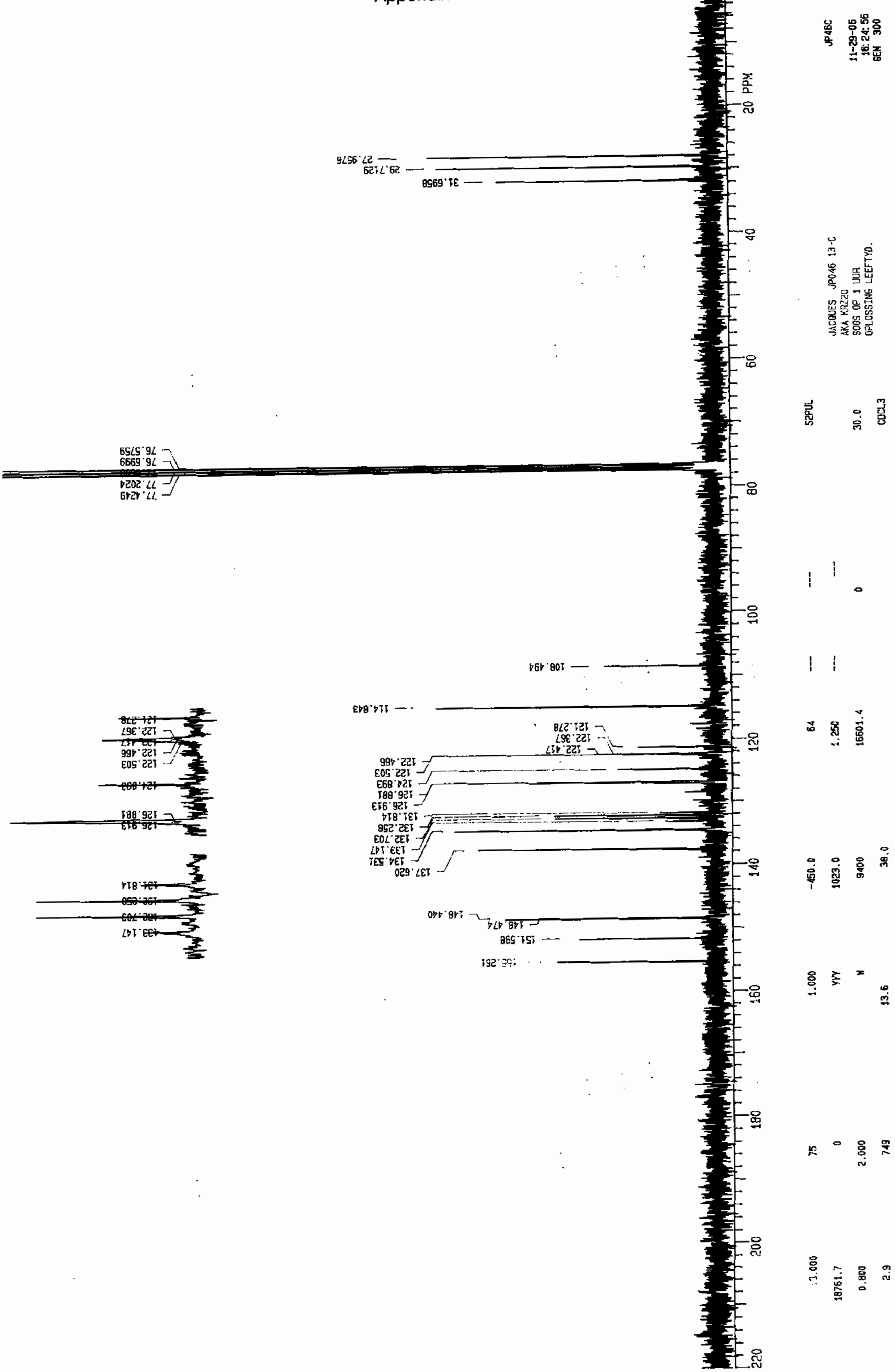
JP46C
11-29-05
16:24:56
GEM 300
JACQUES JP046 13-C
AKA KRZ20
SOGS OP 1 UUR
OPLOSSING LEEFTYD.
52PUL
30.0
CDCL3
PPM
0
20
40
60
80
100
120
140
160
180
200
220
27.9576
29.7129
31.6958
76.5759
76.6999
77.2024
77.4249
108.494
114.843
121.278
122.367
122.417
122.466
122.503
124.893
126.881
126.913
131.814
132.256
132.703
133.147
134.531
137.620
148.440
148.474
151.598
155.261

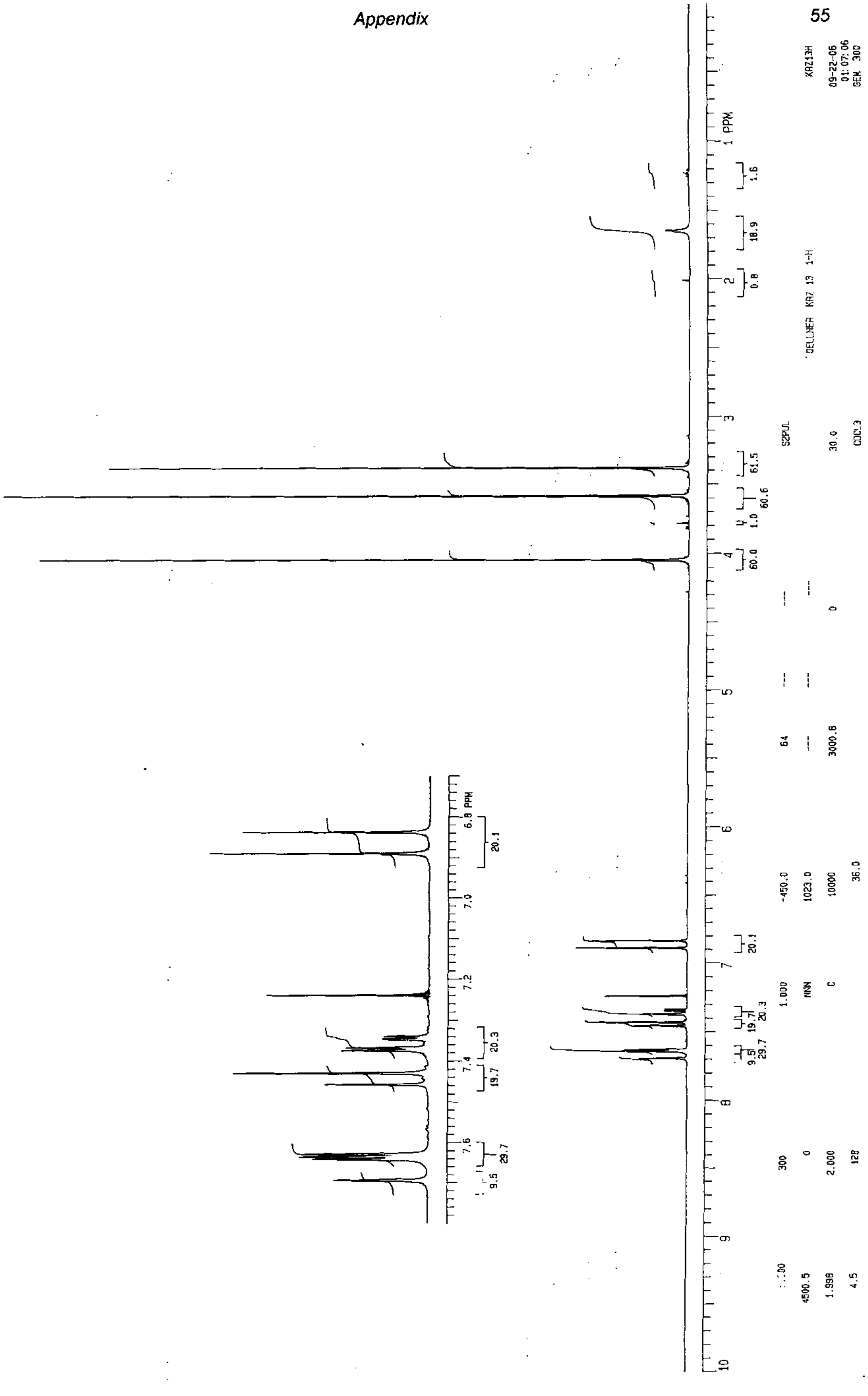
KRZ13H
09-22-06
01:07:06
GEM 300
DELLNER KRZ 13 1-H
S2PUL
30.0
CDCl3
0
64
3000.6
-450.0
1023.0
10000
36.0
1.000
NNN
C
300
0
2.000
128
4500.5
1.998
4.5
PPM
1
2
3
4
5
6
7
8
9
10
1.6
18.9
0.8
61.5
60.6
1.0
60.0
20.1
19.7
20.3
9.5
29.7
6.8
7.0
7.2
7.4
7.6

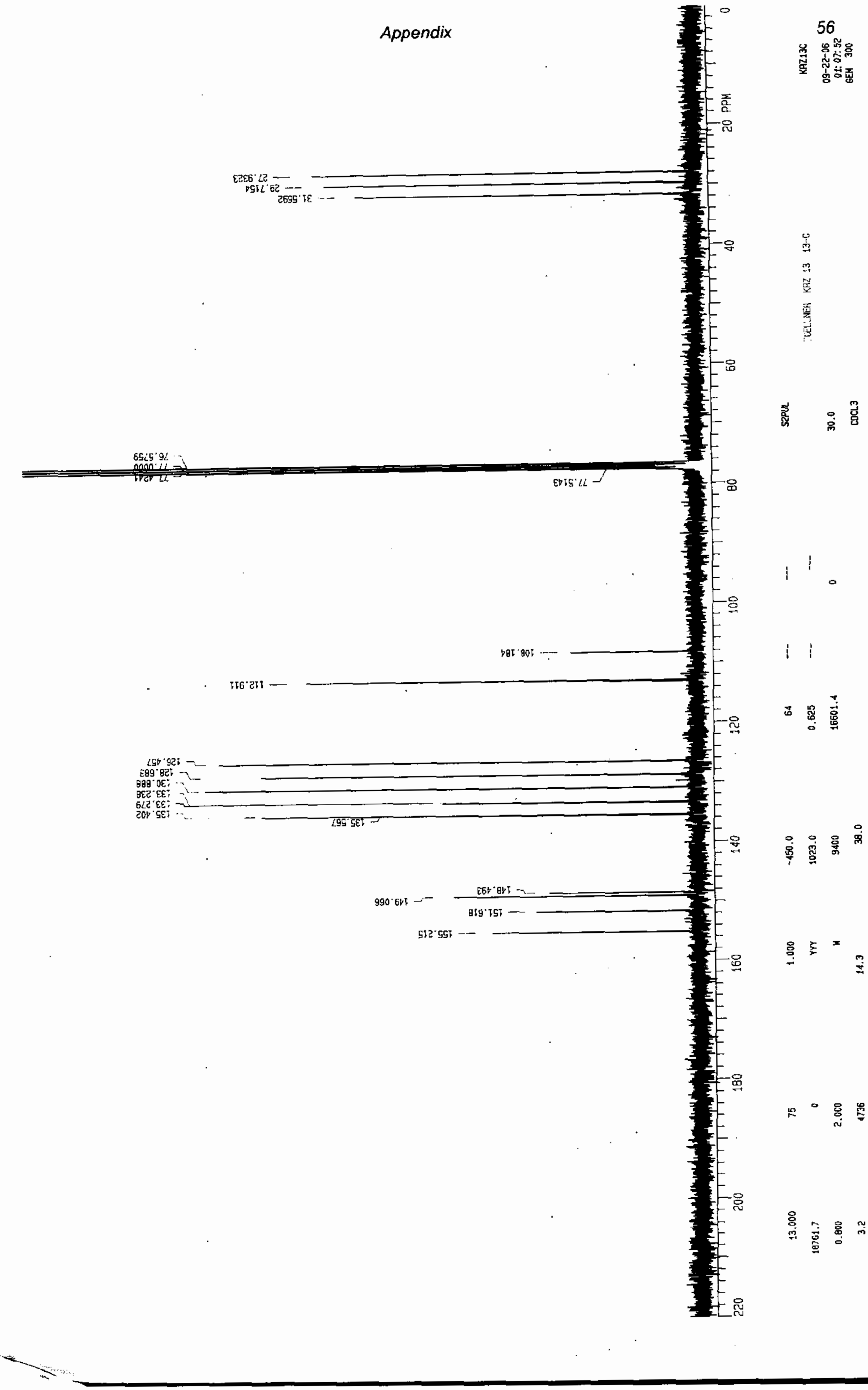
KAZ13C
09-22-06
01:07:52
GEN 300
KELLNER KAZ 13 13-C
S2PUL
30.0
CDCL3
0
64
0.625
16601.4
-450.0
1023.0
9400
38.0
1.000
YYY
N
14.3
75
0
2.000
4736
13.000
10761.7
0.800
3.2
27.9323
29.7154
31.5692
76.5759
77.0000
77.4241
77.5143
108.184
112.911
126.457
128.683
130.888
133.238
133.279
135.402
135.567
148.493
149.066
151.618
155.215
0
20 PPM
40
60
80
100
120
140
160
180
200
220

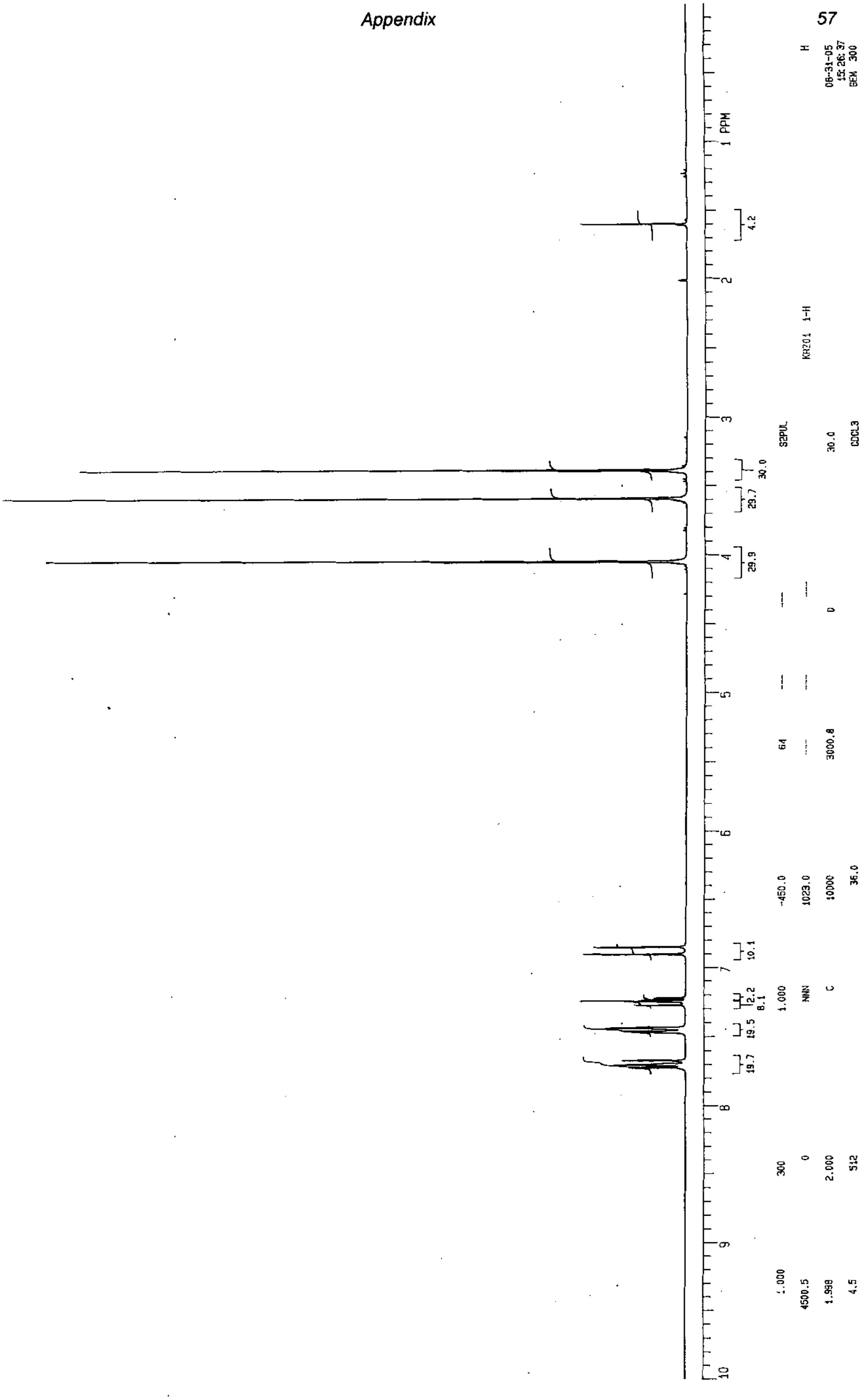
H
08-31-05
15:26:37
GEM 300
KR201 1-H
S2PUL
30.0
CDCL3
0
64
3000.8
-450.0
1023.0
10000
36.0
1.000
NNN
C
300
0
2.000
512
1.000
4500.5
1.998
4.5
1 PPM
2
3
4
5
6
7
8
9
10
4.2
30.0
29.7
29.9
10.1
2.2
8.1
19.5
19.7

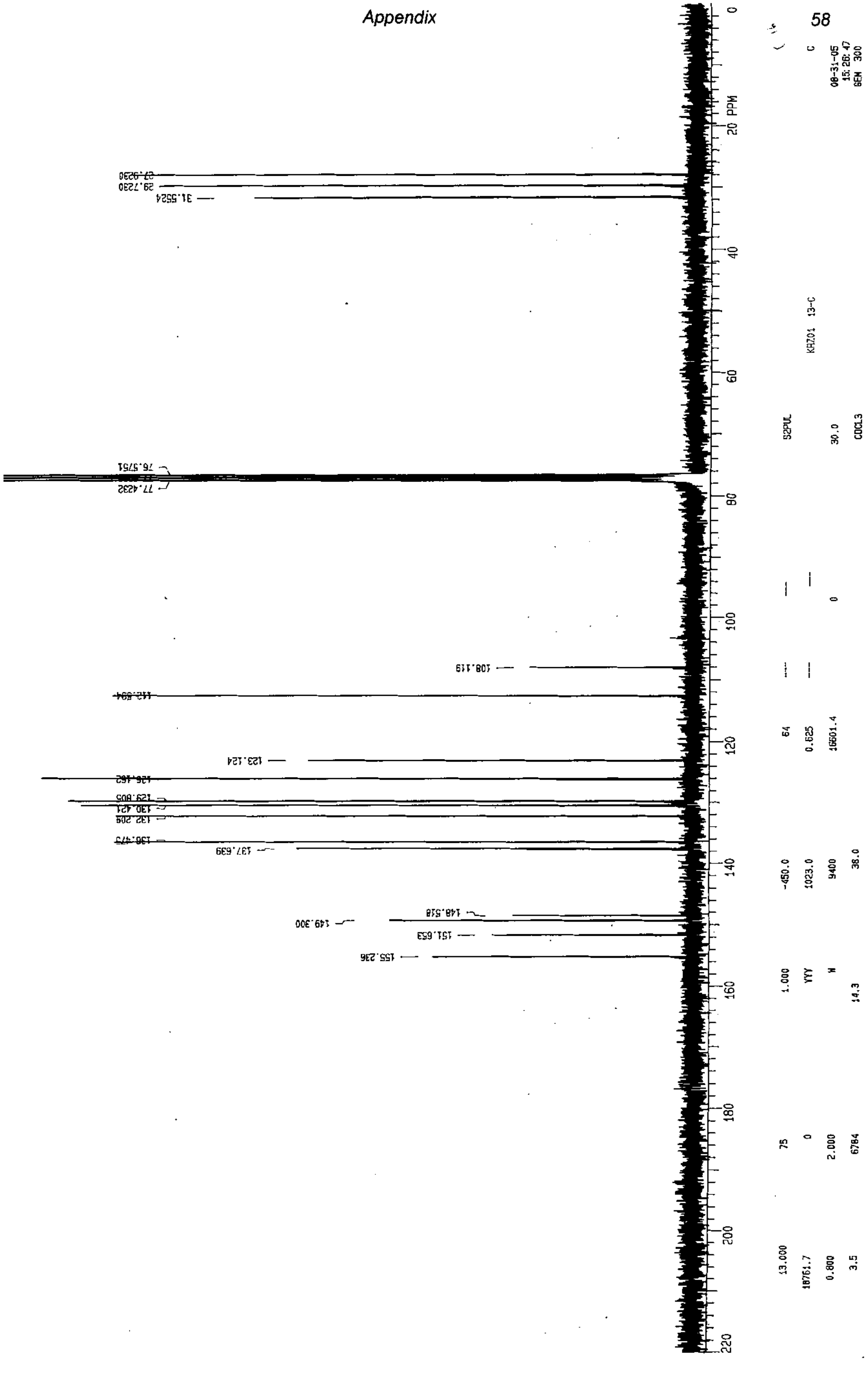
27.9230
29.7230
31.5524
76.5751
77.4232
108.119
112.594
123.124
126.162
129.805
130.421
132.209
136.473
137.639
148.518
149.300
151.653
155.236
0
20 PPM
40
60
80
100
120
140
160
180
200
220
08-31-05
15:26:47
GEM 300
C
KRZ01 13-C
S2PUL
30.0
CDCl3
0
64
0.625
16601.4
-450.0
1023.0
9400
38.0
1.000
YYY
N
14.3
75
0
2.000
6784
13.000
18761.7
0.800
3.5

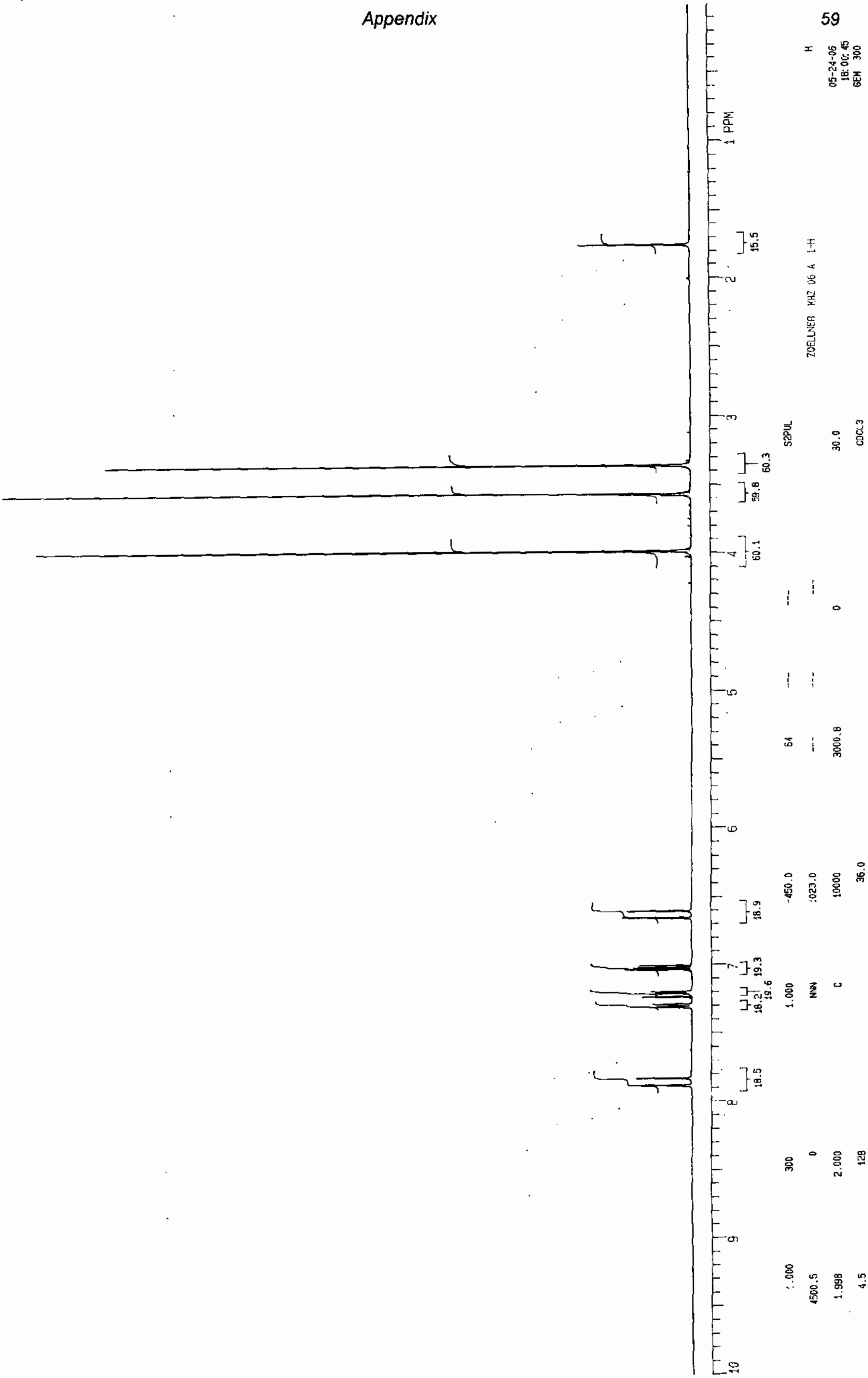
H
05-24-06
18:00:45
GEM 300
ZOELLNER KHZ 06 A 1-H
S2PUL
30.0
CDCL3
1 PPM
2
3
4
5
6
7
8
9
10
15.5
60.3
59.8
60.1
18.9
19.3
19.6
18.2
18.5
0
64
3000.8
-450.0
1023.0
10000
36.0
1.000
NNN
C
300
0
2.000
128
1.000
4500.5
1.998
4.5

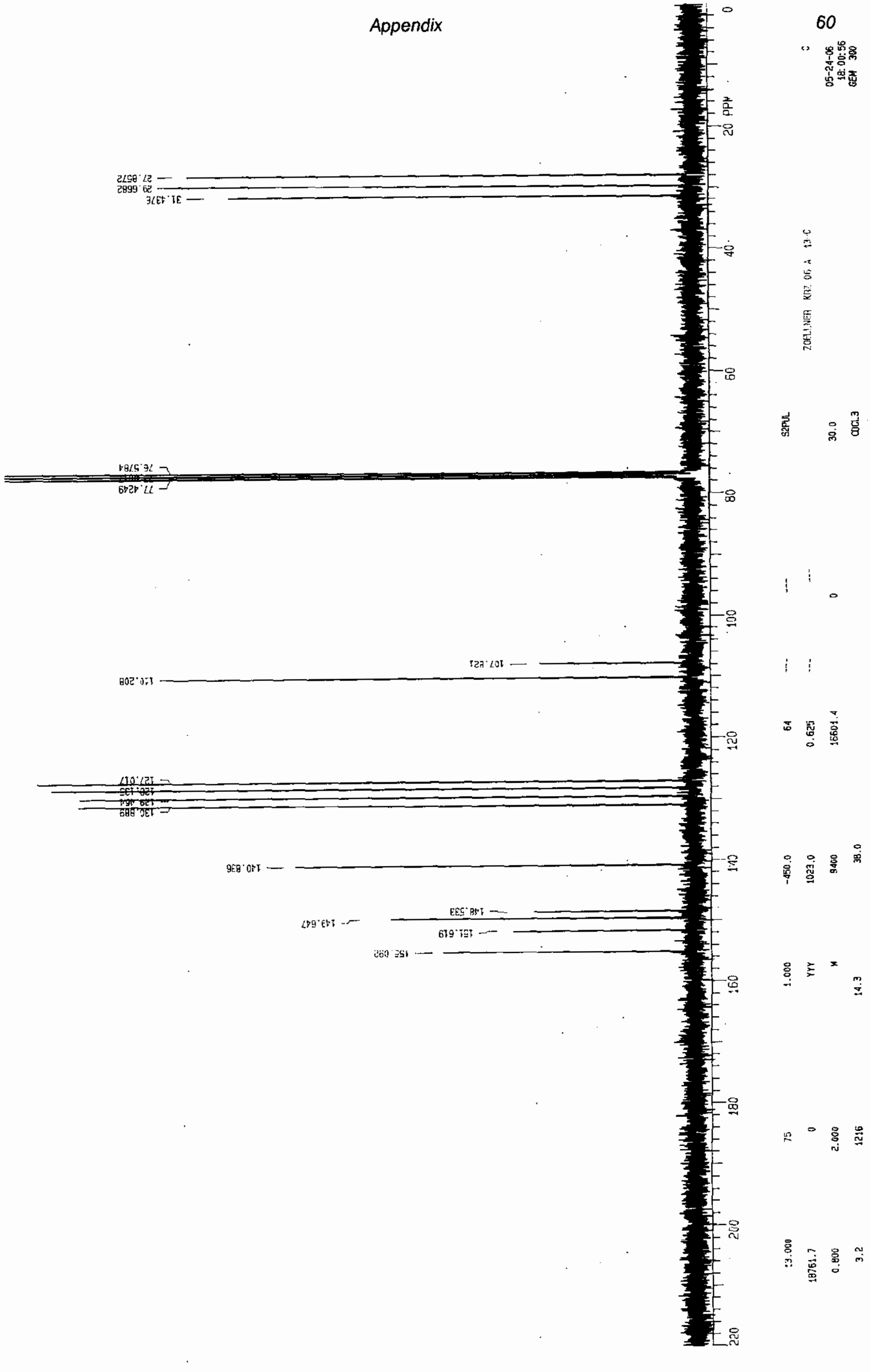
27.8572
29.6682
31.4376
76.5784
77.4249
107.821
110.208
127.017
128.135
129.364
130.889
140.836
148.533
149.647
151.619
152.092
0
20 PPM
40
60
80
100
120
140
160
180
200
220
ZOELLNER KRZ 06 A 13-C
05-24-06
18:00:56
GEM 300
S2PUL
30.0
CDCL3
64
0.625
16601.4
-450.0
1023.0
9460
38.0
1.000
YYY
14.3
75
0
2.000
1216
13.000
18761.7
0.800
3.2

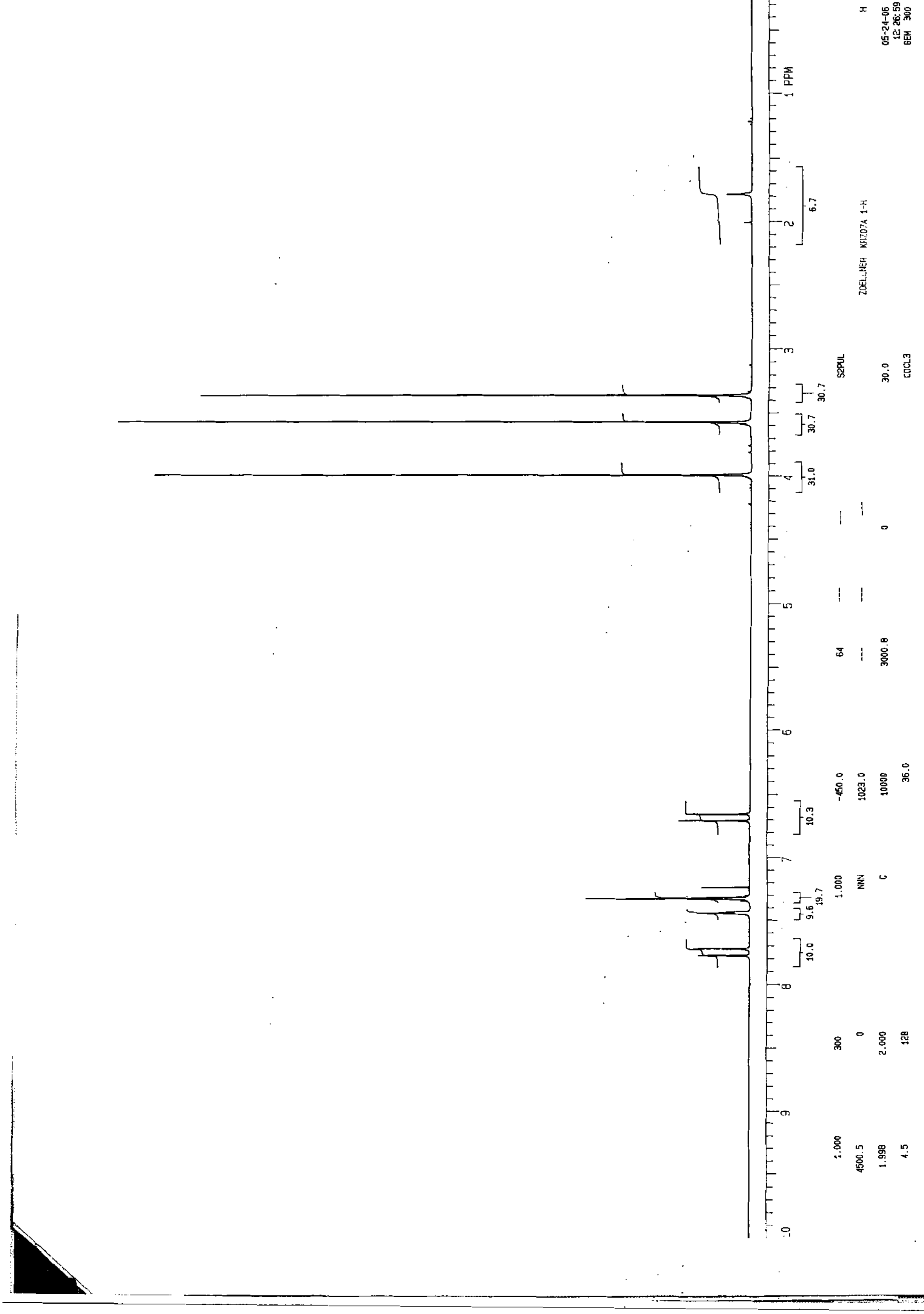
H
05-24-06
12:26:59
GEM 300
ZOELLNER KRZ07A 1-H
S2PUL
30.0
CDCL3
0
64
3000.8
-450.0
1023.0
10000
36.0
1.000
NNN
C
300
0
2.000
128
1.000
4500.5
1.998
4.5
PPM
1
2
3
4
5
6
7
8
9
10
6.7
30.7
30.7
31.0
10.3
19.7
9.6
10.0

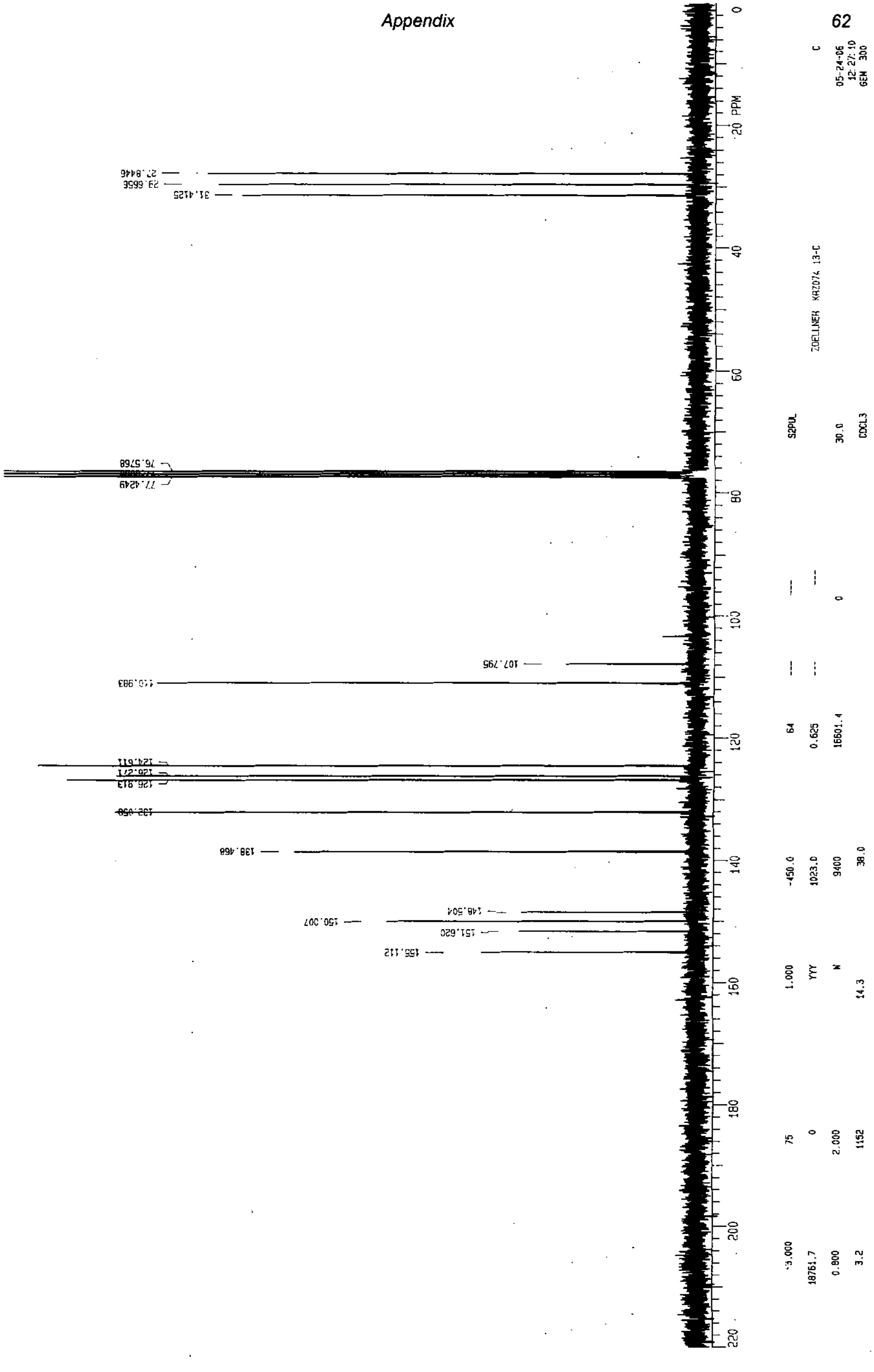
27.8446
29.6656
31.4125
76.5768
77.4249
107.795
110.983
124.611
126.271
126.913
132.058
138.468
148.504
150.007
151.620
155.112
PPM
0
20
40
60
80
100
120
140
160
180
200
220
C
05-24-06
12:27:10
GEM 300
ZOELLNER KRZ074 13-C
S2PUL
30.0
CDCL3
0
64
0.625
16601.4
-450.0
1023.0
9400
38.0
1.000
YYY
N
14.3
75
0
2.000
1152
-3.000
18761.7
0.800
3.2

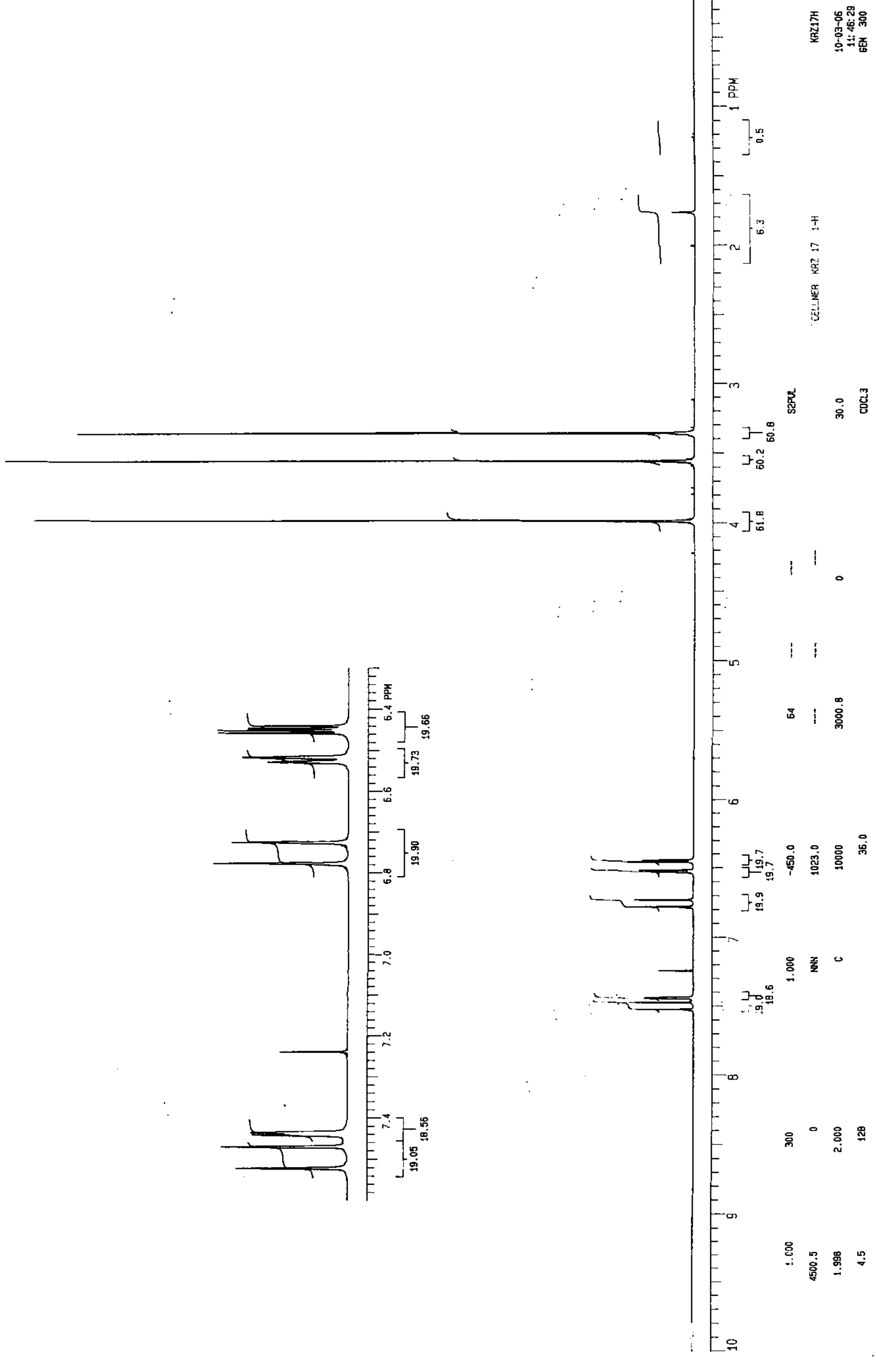
KRZ17H
10-03-06
11:46:29
GEN 300
CELLNER KRZ 17 1-H
S2PUL
30.0
CDCL3
1 PPM
2
3
4
5
6
7
8
9
10
0.5
6.3
60.8
60.2
61.8
19.7
19.7
19.9
19.0
18.6
6.4 PPM
6.6
6.8
7.0
7.2
7.4
19.66
19.73
19.90
19.05
18.56
0
64
3000.8
-450.0
1023.0
10000
36.0
1.000
NNN
C
300
0
2.000
128
1.000
4500.5
1.998
4.5

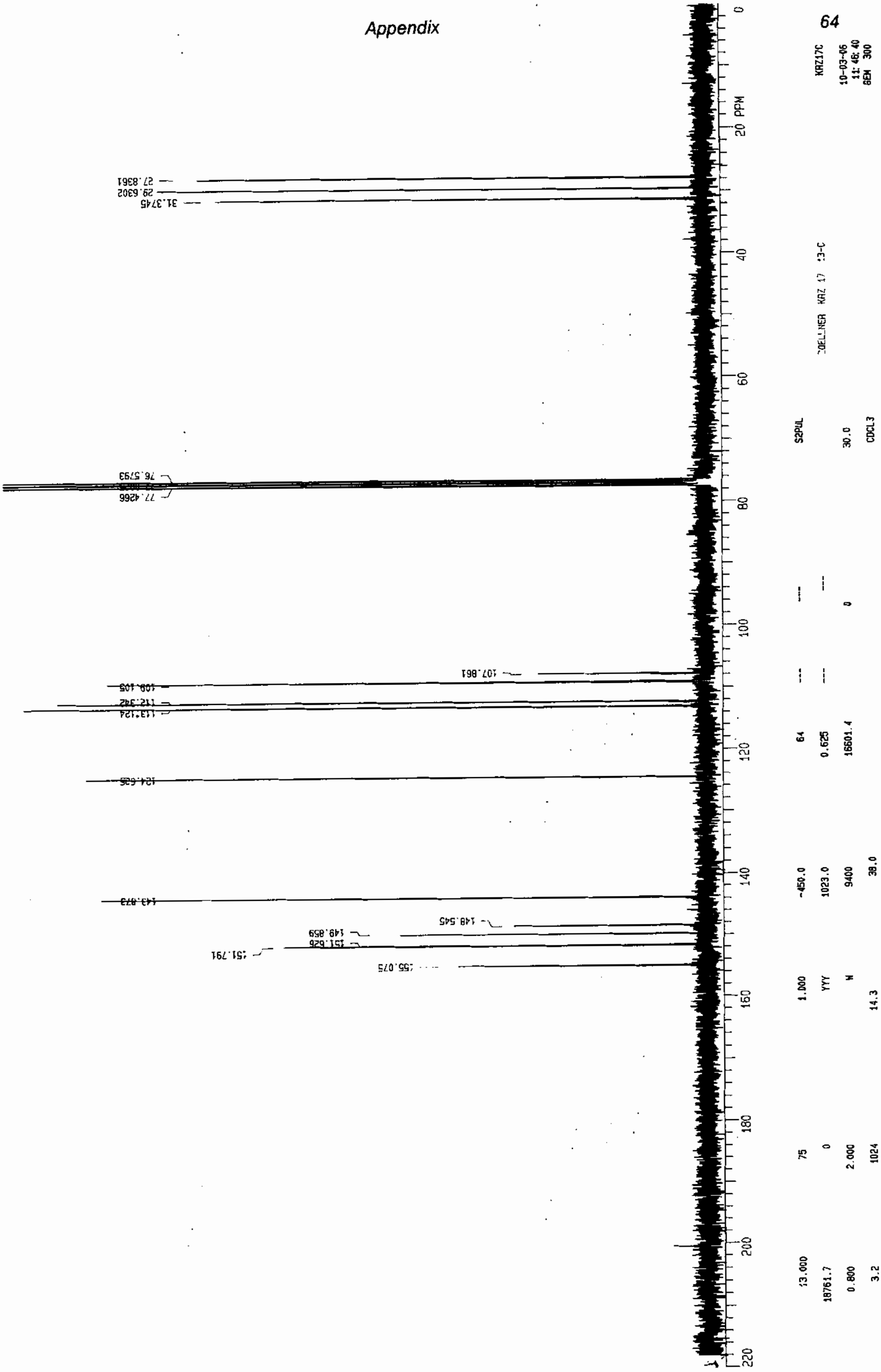
27.8361
29.6302
31.3745
76.5793
77.4266
107.861
109.105
112.342
113.124
124.626
143.873
148.545
148.859
151.626
151.791
155.075
0
20 PPM
40
60
80
100
120
140
160
180
200
220
KRZ17C
10-03-06
11:46:40
BEH 300
ZOELLNER KRZ 17 13-C
S2PUL
30.0
CDCL3
64
0.625
16601.4
-450.0
1023.0
9400
38.0
1.000
YYY
N
14.3
75
0
2.000
1024
13.000
18761.7
0.800
3.2